The Institute of Paper Chemistry

Appleton, Wisconsin

Doctor's Dissertation

A Study of the Diffusion of Sorbed Water Vapor Through Paper and Regenerated Cellulose Films

Arne T. Ahlen

June, 1969

A STUDY OF THE DIFFUSION OF SORBED WATER VAPOR THROUGH PAPER AND REGENERATED CELLULOSE FILMS

A thesis submitted by

Arne T. Ahlen

B.S., 1963, Stanford University
M.S., 1965, Lawrence University

in partial fulfillment of the requirements
of The Institute of Paper Chemistry
for the degree of Doctor of Philosophy
from Lawrence University,
Appleton, Wisconsin

June, 1969

TABLE OF CONTENTS

SUMMARY

It is known that the water-vapor permeability coefficients for paper are generally greater than would be expected from the permeability coefficient of the same sheet to a relatively nonadsorbing gas. The contribution of "sorbed water diffusion" or "bound water diffusion" to the overall permeability coefficient has been determined for many cellulosic materials, but there is no generally accepted mechanism for the transport in the sorbed phase.

The steady-state diffusion of water vapor through paper, regenerated cellulose film, and cellulose acetate film was determined in a constant total pressure diffusion chamber. Small partial pressure differences of water vapor were maintained across the samples and the permeability of a sample to water vapor could be determined at different moisture contents of the sample. The gas-phase diffusion of water vapor through a sample could be calculated from the results of an experiment counterdiffusing two nonadsorbing gases through the sample.

The sorbed vapor permeability (SVP) coefficients, defined as the sorbed water flux divided by the partial pressure gradient of water vapor across the sample, increased rapidly with increasing moisture content for all samples. The SVP coefficients for paper and regenerated cellulose both increased in an exponential manner with increasing mean relative vapor pressure. The similarity in the behavior of sorbed water transport in paper and regenerated cellulose lead to the conclusion that the mechanism of sorbed water transport was the same for these two substances. The cellulose acetate film had a much higher SVP coefficient at low moisture content than did the paper and regenerated cellulose film. The SVP coefficient for cellulose acetate also increased with increasing relative vapor pressure, but this increase was less rapid than for paper and regenerated cellulose film. Over the temperature range 30 to 50°C., the SVP coefficients of paper and regenerated cellulose appeared to be independent of temperature if the values were compared at the same relative vapor pressure.

Most diffusion runs in this study were made at water-vapor pressures less than 70% relative humidity. At these relative humidities, it is not expected that the sorbed transport will be due to capillary driving forces. Equations that have been developed assuming that the sorbed water transport proceeds by surface diffusion in adsorbed monolayers and multilayers did not correlate the sorbed vapor data very well. Surface diffusion theories did not seem to account for several other observations made in this study.

The sorbed water diffusion process seems to be best characterized as proceeding in the amorphous regions of cellulose by a solid-solution diffusion mechanism. The sorbed water disrupts the extensive hydrogen bonding in cellulose, and this results in swelling and increased Brownian motion of the cellulose polymer chain segments in the amorphous regions. Water molecules can diffuse through "holes" formed as the result of the random fluctuation of polymer chain segments. This "activated" diffusion mechanism is the generally accepted theory for the diffusion of gases through polymer films. The same rapid increase in the permeability coefficient with sorbed vapor concentration has been observed when a solvating vapor diffuses through an organic polymer film.

It is not possible from solid-solution diffusion theory to predict what the effect of water-cellulose interaction should be on the sorbed vapor diffusion process. An empirical equation was obtained which did correlate all of the SVP coefficients determined for the paper samples in this study. This equation also fits the data obtained by another investigator who determined the sorbed water vapor transport through paper at different mean vapor pressures.

INTRODUCTION

When a partial pressure difference of water vapor is maintained across a sheet of paper, the result is a net transport of water molecules through the sheet. Part of this transport will be by gaseous diffusion through the pores of the paper. Because water vapor adsorbs on or dissolves in the pulp fiber, two other modes of diffusional transport are possible.

When as adsorbable gas flows through a porous medium under a partial pressure gradient, there will be established a corresponding surface concentration gradient of adsorbed molecules on the solid surface. If the thermal motion of adsorbed molecules does not merely produce vibration about a fixed adsorption site, but endows them also with two-dimensional mobility, they can undergo diffusion along this gradient. The existence of "surface diffusion" in microporous media is well established and has been reviewed by Carman (1).

If the sorbed molecules penetrate into the molecular structure of the medium, it is no longer meaningful to speak of surface diffusion as one does not have distinct surfaces for adsorption. The generally accepted mechanism for the transport of a gas through a polymer film is by dissolution of the gas at the polymer surface, molecular diffusion through the polymer matrix, and finally evaporation of the gas at the other polymer-gas interface (2).

A third mode of sorbed water transport through paper is also possible. If the relative vapor pressure, that is, the vapor pressure of water divided by the saturated vapor pressure is high enough, some of the pores of the paper structure will be filled with capillary condensed water. In a constant total pressure system, the transport of capillary condensed water will be due to capillary pressure forces. This type of flow cannot be treated as diffusional transport.

The purpose of this study was to determine the relative importance of gas-phase and sorbed-phase transport of water in various papers when a partial pressure difference of water vapor is maintained across the sheet. Such information would be useful in determining the mechanisms which govern the removal of water in the final stages of the drying of paper. It is also of interest to those studying the use of paper and paper laminants as packaging materials.

A further purpose of this study was to compare sorbed water transport with models for capillary flow, surface diffusion, and solid-solution diffusion to see what conclusions could be drawn as to the contributions of these different mechanisms to the water transport through paper. A regenerated cellulose film and a cellulose acetate film were also studied to provide comparisons with the sorbed water transport through paper. The important variables which were studied were mean vapor pressure of water vapor and temperature.

LITERATURE REVIEW

WATER-VAPOR PERMEABILITY OF CELLULOSIC MEDIA

It is convenient when studying the transport of gases or vapors through any media to express the results in terms of permeability or diffusion coefficients so that the results of all experiments are reduced to a common basis. The permeability coefficient, P, for a gas or vapor, A, flowing through a porous medium or membrane can be defined quite generally by the following equation:

$$P = N_A/[(p_2 - p_1)/L] \qquad (1)$$

where N_A is the molar flux of the gas or vapor based on the total area of the medium, $(p_2 - p_1)$ is the pressure difference across the medium, and L is the thickness of the medium. For certain mechanisms of transport, the presence of a second gas to maintain constant total pressure does not affect the transport of the gas being studied, and the pressure difference across the medium may be either a total or partial pressure difference without affecting the calculation of the permeability coefficient.

Water-vapor permeability (WVP) coefficients of cellulosic media have previously been determined using both total and partial pressure differences of water vapor. If a total pressure difference is maintained, the flow in the gas phase will be by viscous or laminar flow if the mean free path of the molecule is much less than the average pore diameter of the porous medium, by "free molecule" or Knudsen flow if the mean free path is much greater than the average pore diameter, and by a combination of these if the mean free path is approximately the same as the average pore diameter. In a constant total pressure system, the transport in the gas phase will be by normal diffusion if the mean free path is much less than the average pore diameter. Knudsen flow is really a process of diffusion and takes place for each component of a gas mixture along its own partial pressure gradient. Thus, in the Knudsen region it

makes no difference if the pressure difference is a total pressure difference or a partial pressure difference of one component in a system of constant total pressure. For surface diffusion or solid-solution diffusion, the presence of a nonadsorbing gas should not affect the diffusion of the sorbed species by these mechanisms. The flow of capillary condensed water will be greater when a total pressure difference exists than when the system is at constant total pressure because of an additional viscous flow term.

It is well established that the transport of water vapor through paper cannot always be fully explained in terms of ordinary gas phase flow or diffusion. Vollmer (3) determined the permeability coefficients of dense paper samples to both air and water vapor. He found that the permeability coefficient for water vapor increased rapidly as the mean pressure of water vapor increased. The permeability coefficient increased much more rapidly with mean total pressure than was expected from the results of air permeability measurements for the same sample. Rounsley (4) determined the water-vapor permeability coefficients of a book paper and found that they increased very rapidly above a relative humidity of about 25%.

The transport of water vapor through cellulosic materials with very limited void structure provides a good means of studying sorbed flow phenomena. Stamm studied the water transport through cellophane (5) and metal-impregnated wood (6). He found that the WVP coefficient increased in an exponential manner with increasing mean relative vapor pressure. Since the transport of water vapor through paper and other cellulosic materials cannot be explained solely in terms of gas-phase transport, it follows that there is additional flux in the sorbed phase. This flux might be due to flow of capillary condensed water, surface diffusion of adsorbed water vapor, or diffusion of dissolved molecular water. Only a brief discussion of each of these mechanisms will be given in this section. They will be treated in detail where pertinent in the analysis of results.

CAPILLARY FLOW

In any porous medium, vapor will be sorbed by capillary condensation if the relative vapor pressure is high enough. The Kelvin equation (7) can be used to calculate the radius of a capillary which will be filled by capillary condensate if the relative vapor pressure is raised above a certain value. From thermodynamic considerations the following equation may be derived:

$$\ln (p_A/p_o = \frac{-2\sigma M}{r\rho RT} \qquad (2)$$

where

p_A = partial pressure of A

p_o = saturated vapor pressure (at a plane surface)

σ = surface tension

M = molecular weight

r = radius of the capillary

ρ = density of the liquid

R = gas law constant

T = temperature

Table I gives typical values of r versus relative vapor pressure for water at 25°C. At the lower relative pressures given in Table I, the effective pore radius at which capillary condensation is expected approaches the molecular dimensions of a water molecule. It is doubtful that the Kevin equation is applicable at these low relative pressures or that significant capillary condensation occurs.

In a constant total pressure system, capillary flow is caused by capillary forces. In a pore filled with liquid, the pressure difference causing flow is related to the curvatures of the interfaces at the two ends of the liquid-filled pore. Small differences in the partial vapor pressures at the two interfaces will result in large pressure

gradients in the capillary-held liquid. Thus, the transport of water molecules through a liquid-filled capillary would be very rapid.

TABLE I

EFFECTIVE CAPILLARY RADIUS CALCULATED FROM KELVIN EQUATION FOR WATER AT 25°C.

Relative Vapor Pressure, p_A/p_o	Effective Capillary Radius, μm.
0.99	0.106
0.95	0.020
0.90	0.010
0.80	0.0044
0.70	0.0029
0.60	0.0020
0.50	0.0015

SURFACE DIFFUSION

That molecules physically adsorbed on a solid surface may be mobile has been recognized since 1925 when Volmer and Adhikari (8) demonstrated that surface molecules of benzophenone are mobile. Carman (1) has extensively reviewed the subject of surface diffusion in porous media, and he gives an excellent description of the nature of surface diffusion.

There are two types of surface mobility to be distinguished. If a solid surface is completely uniform, there are no specific adsorption sites and therefore no barriers to the movement of an adsorbed molecule. In very dilute monolayers, at least, the adsorbed molecule would be expected to behave as a two-dimensional gas. Carman (1) states that both the concentration and temperature dependence of observed surface diffusion coefficients do not support this model. The solid surface can also be considered to have definite adsorption sites with energy barriers between sites. If a molecule gains energy equal to the heat of adsorption, it becomes desorbed, but

smaller energies might enable it to jump from one site to another without leaving the surface. Surface mobility by such a "hopping" mechanism would lead to a net flux if a concentration gradient of adsorbed molecules existed on the solid surface. This type of "activated diffusion" is not inconsistent with the observed temperature dependence of surface diffusion coefficients reported by Carman (1). In general, surface diffusion coefficients obey the Arrhenius relationship of temperature dependence for an activated process.

There are basically two approaches to the quantitative description of the surface diffusion process. One attempts to formulate expressions for the frequency of "jumps" to a neighboring adsorption site and for the average distance traveled in a "jump," and the other uses the concept of a "spreading pressure" of adsorbed molecules. The derivation of Weaver and Metzner (9) is representative of the former approach. They derive expressions for mean hopping rate and mean hopping distance which give the pressure and surface concentration dependency of surface transport explicitly. Only two experimental determinations are needed to evaluate partition functions and activation energy. So far, this approach has been limited to systems with less than full monolayer coverage and with energetically smooth surfaces.

The spreading pressure of a monolayer film on a liquid substrate can be measured directly with a surface balance. When the underlying phase is solid, one cannot directly measure the spreading pressure, but it is still a useful concept. Fowler and Guggenheim (10) present statistical derivations for the spreading pressure of mobile and ideal localized monolayers. They define a mobile monolayer as one being composed of adsorbed molecules which are bound tightly to the solid surface in the normal direction but which have complete freedom of movement in the two directions of the surface. The two-dimensional spreading pressure, ϕ, for a mobile monolayer is given by

$$\phi = NkT \qquad (3)$$

where N is the number of molecules adsorbed per unit area and k is Boltzmann's constant. An ideal localized monolayer is composed of adsorbed molecules located on definite sites on the solid surface. The spreading pressure for this type of monolayer is given by

$$\phi = N_o kT \ln\left(\frac{1}{1 - \theta}\right) \qquad (4)$$

where N_o is the number of adsorption sites per unit area and θ is the fraction of sites occupied.

Babbitt (11) proposed that the spreading pressure is the driving force for surface diffusion. He assumed that the average velocity of adsorbed molecules, u, over the solid surface is related to the spreading pressure by the following equation:

$$\frac{d\phi}{dz} = -C_R u \qquad (5)$$

where C_R is the coefficient of resistance and z is the direction of flow. This equation has been used by Babbitt (11), Gilliland, et al. (12), Bell and Brown (13), and Rounsley (4) as the basis for deriving expressions for the flux due to surface transport.

SOLID-SOLUTION DIFFUSION

The generally accepted mechanism for the diffusion of a gas molecule dissolved in a polymer matrix is by an activated jump through "holes" resulting from random, thermal motion of polymer chain segments. A molecule dissolved in the polymer may move or "jump" from one position to another if the motion of the macromolecule segments are such that there is momentarily a vacant space large enough to accommodate the diffusing species. The ability of polymer chain segments to move cooperatively to produce a decreased local density is responsible for the movement of dissolved gas

molecules in the polymer matrix and, hence, for the net transport of gas molecules through the film when a concentration gradient exists. If there is no appreciable interaction between the dissolved molecules and the polymer, the diffusion process at a given temperature depends primarily on the molecular size of the diffusing species.

In general, the diffusional flux of a molecular species through a membrane is given by the product of three terms, namely, concentration, driving force, and a proportionality factor. The thermodynamic driving force for diffusion is the chemical potential, μ (14). In terms of this driving force, the flux is given by

$$N_{As} = \frac{D_s}{RT} c_s \left(- \frac{d\mu}{dz} \right) \tag{6}$$

where N_{As} is the sorbed vapor flux, c_s is the molar sorbed vapor concentration, and D_s is the diffusion coefficient. Since $\mu = \mu_* + RT \ln a$, where a is the activity,

$$N_{As} = -D_s c_s \left[\frac{d(\ln a)}{dz} \right] . \tag{7}$$

Substituting for $a = \gamma c_s$ where γ is the activity coefficient,

$$N_{As} = -D_s \left[\frac{dc_s}{dz} + c_s \frac{d \ln \gamma}{dz} \right] . \tag{8}$$

For a sorbed phase which follows Henry's law, the second term inside the brackets is zero and Equation (8) reduces to Fick's first law:

$$N_{As} = -D_s \frac{dc_s}{dz} . \tag{9}$$

Fick's first law is generally assumed when calculating diffusion coefficients for gases through polymers. For many polymer-gas systems the diffusion coefficients calculated using Fick's first law are not dependent on concentration.

Fick's first law is usually also assumed for surface diffusion. The dependence of this diffusion coefficient on concentration is then empirically related to other factors which affect the surface diffusion process. A Fick's law diffusion coefficient can be calculated for capillary flow, but this has no physical meaning.

GAS-PHASE DIFFUSION

Matters (15) derived the following equation for the steady-state, normal counter-diffusion of two ideal gases, A' and B', through a porous medium under conditions of uniform temperature and pressure:

$$N_{A'} = [(D_{A'B'})_e p/(\alpha RTL)] \ln [(1 - \alpha y_{A'L})/(1 - \alpha y_{A'0})] \qquad (10)$$

where

$(D_{A'B'})_e$ = effective normal diffusion coefficient

p = total pressure

$r_{A'B'}$ = flux ratio, $N_{B'}/N_{A'}$

α = $1 + r_{A'B'}$

$y_{A'L}$ = mole fraction of A' at $z = L$

$y_{A'0}$ = mole fraction of A' at $z = 0$

The molar flux, $N_{A'}$, is based on the overall cross-sectional area of the porous medium. The effective normal diffusion coefficient embodies all of the structural effects of the porous medium on the diffusion resistance as well as the molecular properties of the gas. If the gas-phase diffusion is in the Knudsen region, the flux is given by

$$N_{A'} = [(D_{KA'})_e p/RTL](y_{A'0} - y_{A'L}) \qquad (11)$$

where $(D_{KA'})_e$ is the effective Knudsen diffusion coefficient. When the effective pore diameter of the porous medium is approximately equal to the mean free path of the gas molecules, the nature of the diffusion process will be intermediate between that of normal diffusion and that of Knudsen diffusion.

For steady-state counterdiffusion of two gases through a porous medium, the flux ratio, $N_{B'}/N_{A'}$, is of interest. For Knudsen diffusion, it can be shown that

$$N_{B'}/N_{A'} = (M_{A'}/M_{B'})^{1/2} \qquad (12)$$

where $M_{A'}$ and $M_{B'}$ are the molecular weights of species A' and B', respectively. Equation (12) follows because the Knudsen diffusion coefficient is directly proportional to the mean molecular speed, $\bar{u}_{A'}$, and $\bar{u}_{A'}/\bar{u}_{B'} = (M_{B'}/M_{A'})^{1/2}$.

On the basis of negligible molecule-wall collisions, McCarty and Mason (16) showed that the mass average velocity of the gas is zero for the counterdiffusion of two gases through a capillary at constant total pressure. This leads to the flux ratio being equal to $M_{A'}/M_{B'}$. This upper limit has never been observed for the counterdiffusion of gases through porous media. For porous media studied so far the flux ratio was found to be close to $(M_{A'}/M_{B'})^{1/2}$ for the normal, the intermediate, and the Knudsen regions (17-19).

Thus, a deviation of the counterdiffusion of two gases from the behavior predicted by Equation (12) could be interpreted as augmented flux of one species due to sorbed transport.

To separate the contribution of transport in the gas phase from that in the sorbed phase, it is convenient to define a new term. The diffusibility, δ, has been defined as the ratio of the effective diffusion coefficient to the true diffusion coefficient (17). The true diffusion coefficient may be thought of as that diffusion coefficient obtained for the same process of diffusion through a uniform, straight capillary whose radius is equivalent to the average pore radius of the porous medium. The diffusibility is dependent on the geometric properties of the porous medium and may be used to calculate the effective diffusion coefficients of different gases through the same medium. The diffusibility accounts for the presence of the solid

fraction of the porous medium through which the gas molecules cannot diffuse and also for the longer path that the molecules must diffuse along.

For normal diffusion, the diffusibility is given by

$$\delta = (D_{A'B'})_e / D_{A'B'} \tag{13}$$

where $D_{A'B'}$ is the binary diffusion coefficient taken from the literature or calculated from the Chapman-Enskog formula, and $(D_{A'B'})_e$ is the effective normal diffusion coefficient determined experimentally for the two nonadsorbing gases. The effective normal diffusion coefficient for another gas pair, A and B, counterdiffusing through the same medium can be calculated from Equation (13) using the binary diffusion coefficient of the new gas pair. If A is an adsorbable gas and it is assumed that the gas-phase and sorbed-phase transport proceed independently of one another,

$$N_{As} = N_A - N_{Ag} \tag{14}$$

where N_{As} is the flux in the sorbed phase, N_A is the measured total flux of A, and N_{Ag} is the gas-phase flux calculated from Equation (10) using the effective normal diffusion coefficient calculated from the diffusibility.

For Knudsen diffusion, the ratio of the effective Knudsen diffusion coefficients of two different gases is given by

$$\frac{D_{KA}}{D_{KA'}} = \frac{(D_{KA})_e}{(D_{KA'})_e} = \left(\frac{M_{A'}}{M_A}\right)^{1/2} \tag{15}$$

If the diffusion of an adsorbable gas, A, proceeds independently in the gas and sorbed phases, the contribution to the total flux of each phase can be determined if the effective Knudsen diffusion coefficient of a nonadsorbing gas, A', is known.

EXPERIMENTAL EQUIPMENT AND TECHNIQUES

PRELIMINARY CONSIDERATIONS

As stated previously, this study was concerned with the transport of water molecules through porous media of cellulose substructure when a partial pressure difference of water vapor was maintained across the sample. Since the transport of water vapor through paper may be strongly dependent on the mean relative vapor pressure at which the experiment is carried out, it was desirable to be able to make measurements at small partial pressure differences over a wide range of mean partial pressures. To calculate the diffusional flux of water vapor in the gas phase, it was also desirable to be able to measure the diffusion resistance of the sample to nonadsorbing gases with the same system.

A diffusion cell which could be adapted for this study had been built by Matters (15). Matters' flow system allowed both sides of the sample to be swept by gas streams of known composition and flow rate. Analysis of the exit streams permitted the calculation of the steady-state fluxes through the sample. In this study, two nitrogen streams were conditioned to known concentrations of water-vapor content. The concentration of water vapor in either stream could be varied from 0 to 80% relative humidity. Argon and nitrogen were used when two nonadsorbing gases were required. Several experiments were made with carbon dioxide and nitrogen to check results reported by Matters.

Experiments on the counterdiffusion of nitrogen and water vapor through nylon fiber beds were made because Matters (15) had reported significant surface diffusion of carbon dioxide when studying the counterdiffusion of nitrogen and carbon dioxide through nylon fiber beds. When it was found that the diffusion of water vapor and of carbon dioxide through nylon fiber beds could be interpreted in terms of ordinary

gas-phase diffusion, the diffusion cell was modified further so that paper sheets and cellulose films could be studied.

DIFFUSION STUDIES

DIFFUSION CELL

The diffusion cell used in this study has been described by Matters (15). Basically, the diffusion chamber consists of two identical half-cells for the entrance and exit of the gases which sweep the two sides of the porous medium or membrane to be studied. A sectional view of one half-cell is shown in Fig. 1. Each half-cell consists of two brass, concentric cylinders. The inner cylinder is the test area and has a diameter of 3.00 inches. The outer cylinder functions as a guard ring to minimize complications due to the leakage of gas around the edge of the test specimen. The diffusion measurements were concerned only with the area within the inner or test cylinder. Gas entered each cylinder through manifolds (A and A') and sets of 12 circumferential holes. Exit of the gas streams took place through similar sets of circumferential holes and manifolds (B and B').

Uniformity of total pressure throughout the entire diffusion chamber is one of the most important factors in the operation of this diffusion system. Pressure taps (C and C') were located on both gas cells to monitor total pressure and pressure differences between chambers.

For studying thick mats (1.191 cm.), a 5-inch diameter retaining ring (E) was used. The mats were confined between brass septums (D and D') located close to the gas entrance ports in each half-cell. The septa had interspersed 0.18-inch holes to give an open area of about 55%. For study of paper sheets and polymer films, the equipment was modified slightly. The septa were removed and the sample to be studied was placed between two gaskets cut from 3/16-inch silicone rubber. The gaskets had

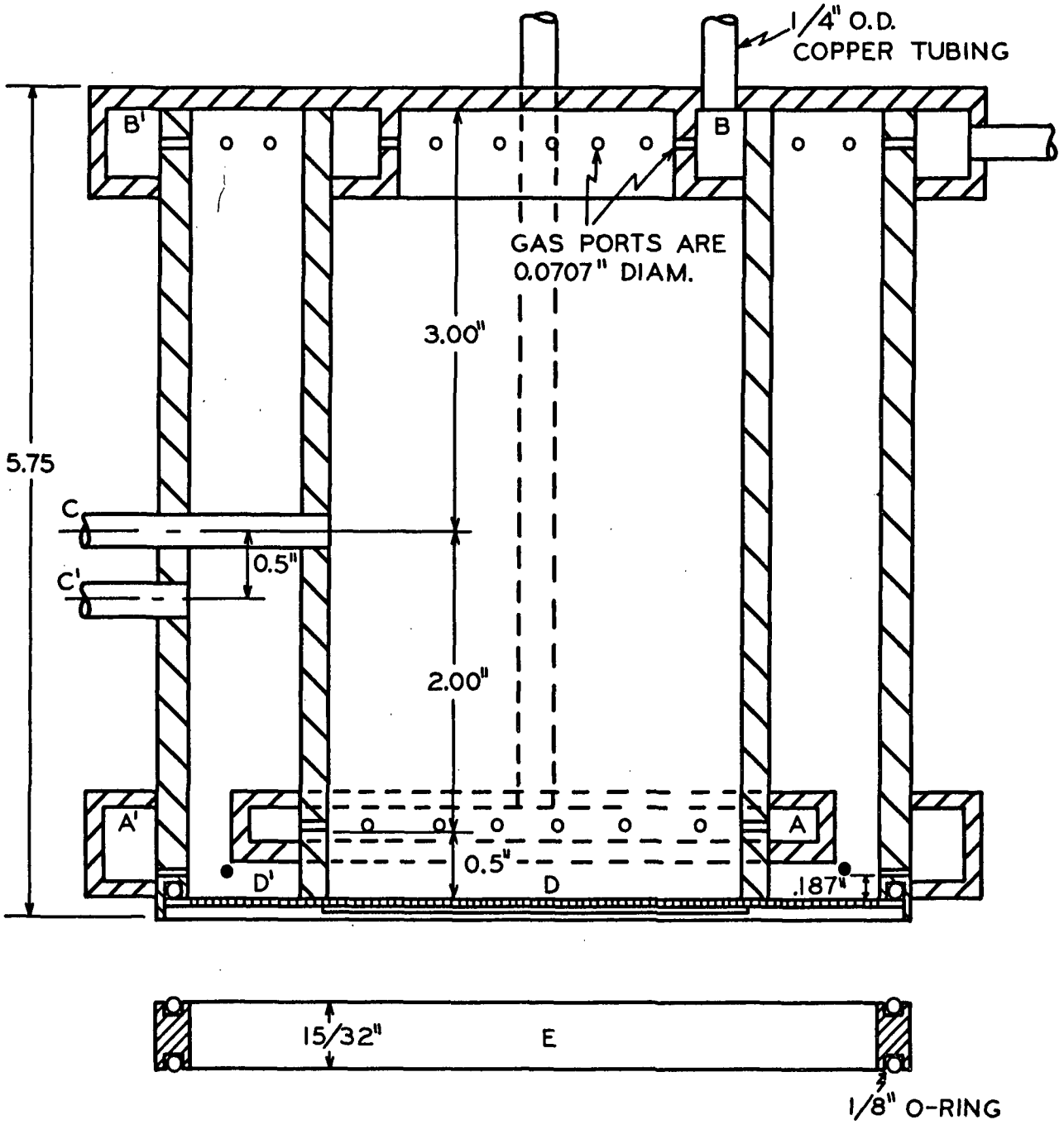

Figure 1. Top Half-Cell of Diffusion Chamber (Full Scale)

a 3.00-inch inner diameter and a 5-3/16-inch outer diameter. When the sample holder was placed between the two halves of the diffusion cell, air-tight seals were formed both at the inner and outer cylinders. Clamping together of the two half-cells was provided for by three steel rods which extended from the bottom plate of a stand to a removable plate on top of the chamber.

PRESSURE BALANCING

Matters used inclined manometers filled with dioctyl phthalate to monitor differences in pressures between chambers of the diffusion cell. In his experiments, he found that pressure differences between the two test chambers as small as 13 dynes/cm.^{2} could lead to significant forced flow. Since the sensitivity of the inclined manometer was only slightly better than 7 dynes/cm.^{2}, the inclined manometers were replaced by a micromanometer built by Reeves (20) according to a design given by Eichorn and Irvine (21). A schematic drawing outlining the principle of operation is shown in Fig. 2. It consists of concentric cylinders placed in manometer fluid (dioctyl phthalate) and capped at the top. A mirrored float, hinged in the inner chamber, provides remote indication of fluid level by means of suitable optical devices. A micrometer connected to a rod of known diameter is used for calibration. It was determined that pressure differences as small as 0.1 dyne/cm.^{2} could be detected with this instrument. This high sensitivity was the result of having a very long optical lever arm (about 10 feet).

FLOW SYSTEM

To carry out diffusion studies, the system had to contain facilities for controlling and monitoring temperature, flow rates, pressures, pressure differences, and gas compositions. The flow system and its various components are schematically illustrated in Fig. 3. Since the guard ring apparatus was not used in the major experiments, the flow system to it is not shown.

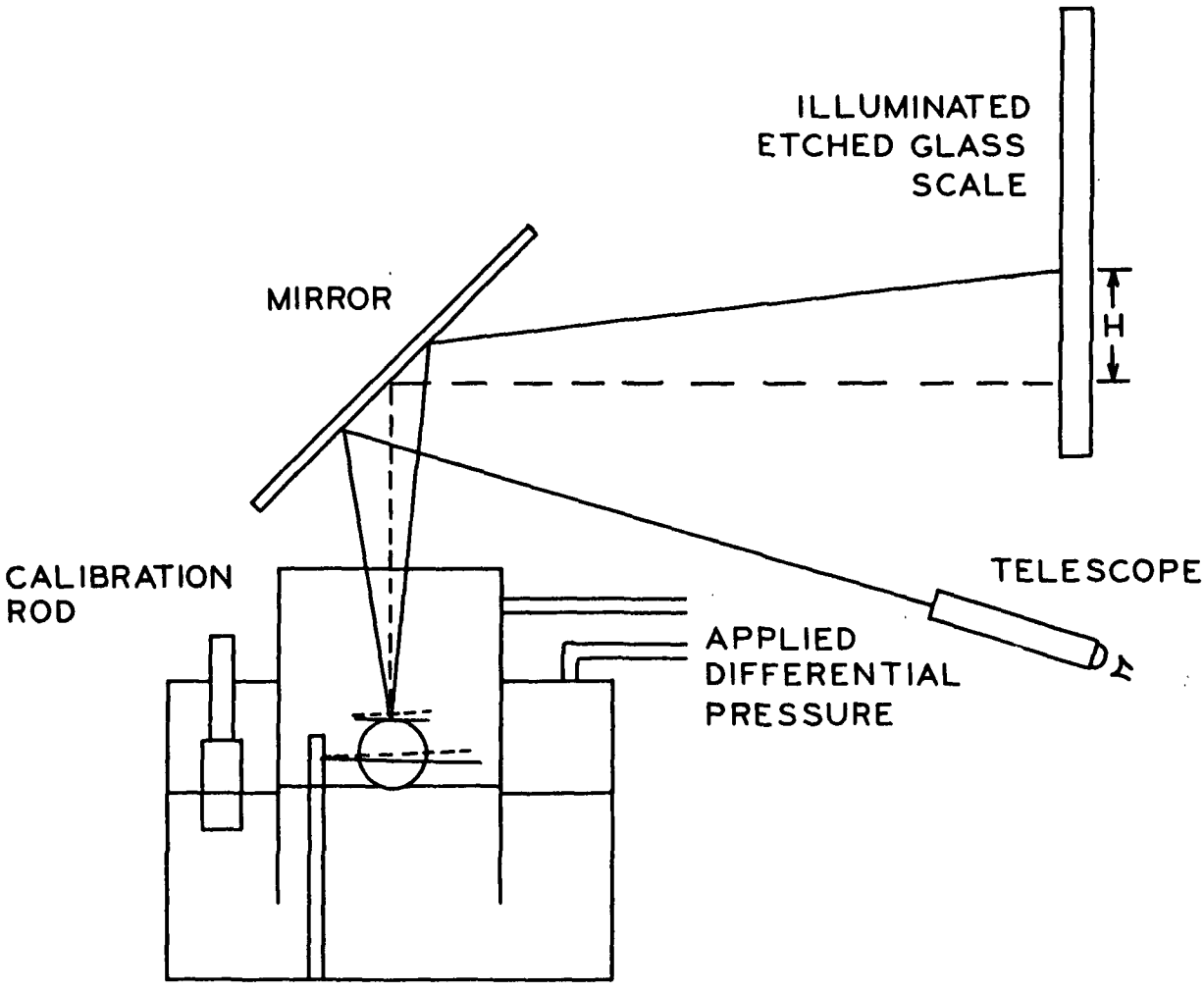

Figure 2. Micromanometer; Schematic Diagram Illustrating Principles of Operation

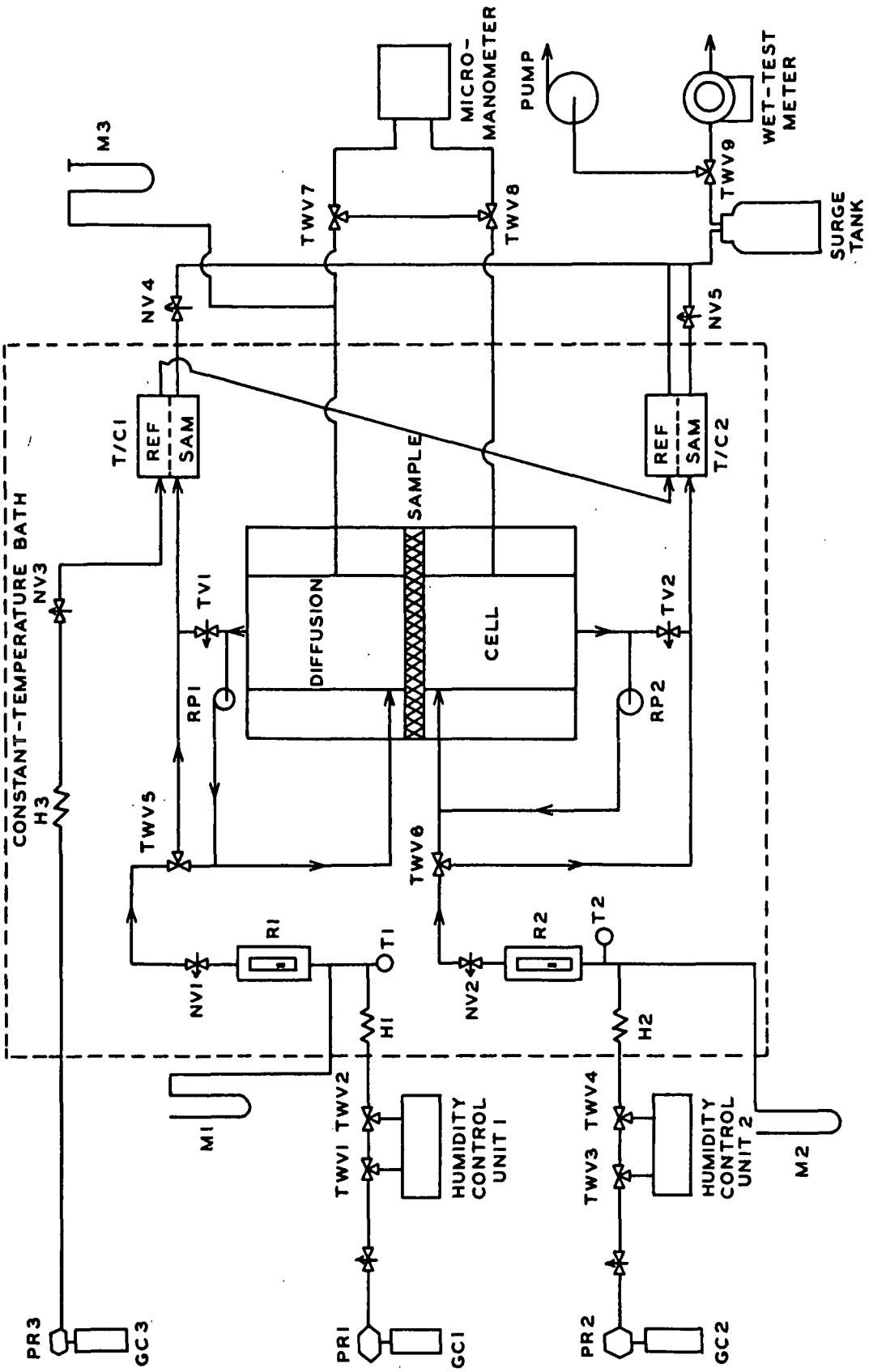

Figure 3. Flow Diagram of Diffusion System

Gas flows flows from the storage cylinder (GC1 or GC2) through a pressure regulator (PR1 or PR2). The gas stream can then flow through a humidity control unit or by-pass it by means of three-way stopcocks (TWV1 and TWV2). The stream is then heated up to the temperature of the constant air bath by passing through 20 feet of 1/4-inch copper tubing (H1 or H2). A thermocouple (T1 or T2) is used to monitor the temperature of the incoming stream. The stream flows through a rotameter (R1 or R2) to a needle valve (NV1 or NV2) which is used to control the flow rate to the diffusion cell. The gas flows through the inlet manifold of the diffusion cell and mixes with the gas diffusing through the porous medium or membrane. The mixture flows out through the exit manifold and through the thermal conductivity (T/C) cell (T/C1 or T/C2) used to analyze the composition of the exit stream. From the T/C cell, the gas flows through a 5-gallon surge tank to a wet-test meter used for calibrating the rotameters and measuring total gas flow. A three-way valve (TWV9) allows the flow system to be evacuated with a high vacuum oil pump.

For zero balancing the T/C cells, three-way valves (TWV5 and TWV6) can direct the flow through a by-pass line around the diffusion cell to the T/C cells. Toggle valves TV1 and TV2 were closed during zero balancing. Diaphragm pumps (RP1 and RP2) were placed in the system when it was found that stagnant air layers were significantly contributing to the measured diffusion resistance for the sweep gas velocities that Matters used. The Universal Electric diaphragm pumps took part of the exit stream from the diffusion cell and recycled it back to the inlet stream to increase the velocity of the gas through the inlet manifold ports. Small surge bottles (500 ml.) were located before and after the diaphragm pump to minimize pressure surges to the diffusion cell, and rotameters were used to determine the recirculation rate. In addition to the pumps, thin strips of brass shim stock were attached to the inside of the test cylinders. These strips deflected the gas streams from the inlet manifold

ports toward the sample being studied and resulted in better mixing of the inlet gas streams with the gases diffusing through the sample.

Fischer-Porter triflat rotameters were used. They were calibrated with a Precision Scientific "Precision" wet-test meter. The pressures upstream from Rotameters R1 and R2 were measured with mercury-filled manometers (M1 and M2) and were regulated by the pressure regulators (PR1 and PR2). Barometric pressure was measured by an Airguide aneroid barometer. Throughout the calibration of these rotameters, the upstream pressure was maintained at 1000 $\pm$ 1 mm. Hg absolute. The rotameters were found to have the approximate flow range 0.50-20.0 std. cc./sec. Duplicate flow-rate determinations differed by 1% or less. During the course of this study, considerable difficulty was encountered with contamination in Rotameters R1 and R2. Because of this, the "Precision" wet-test meter was used to check the flow rates in all experiments reported in this thesis. When steady state had been reached, the total flow of gas from the diffusion cell was measured with the wet-test meter. Then one of the inlet streams was shut off and the flow rate of the other stream measured with the wet-test meter. The flow rate of the first stream was calculated by difference. The precision of the wet-test meter was better than 0.5% at the flow rates used. The calibration of the wet-test meter was checked by liquid displacement and found to be accurate within 1%.

Operation of the system under uniform temperature conditions was provided for by a thermostatically controlled air bath. The air bath is described by Matters (15). The Fenwal thermoregulator was replaced by a platinum-in-mercury thermoregulator to give better temperature control. The temperature of the flowing gases could be maintained to $\pm$ 0.02°C. of the set point. The maximum point-to-point variation of the air temperature bath was found to be about 0.5°C.

The thermal conductivity cells used to determine the composition of the exit streams have been described by Matters (15). Thermal conductivity gas analyzers

detect changes in the thermal conductivity of a gas and therefore changes in its composition as a function of the change in resistance of an electrically heated wire or thermistor. Operation of the thermal conductivity cells depends on balancing a Wheatstone bridge circuit when the reference and sample filaments of the T/C cell are surrounded by a reference gas and then measuring the out-of-balance potential when the sample filament is exposed to the sample gas.

In the present study, the electrical equipment and circuit were the same as described by Matters (15). A slightly different gas flow scheme and calibrating procedure were used. An additional nitrogen cylinder (GC3) was used to supply gas to the reference filaments of the two T/C cells. The T/C cells were zero balanced by passing pure nitrogen from two other gas cylinders (GC1 or GC2) through the sample passages of the T/C cell. To calibrate the T/C cells for either nitrogen and argon or nitrogen and carbon dioxide, the diffusion cell was assembled without a sample. The nitrogen and argon or carbon dioxide from gas cylinders GC1 and GC2 flowed into the diffusion cell and the combined streams were made to flow to one of the two T/C cells by closing needle valve NV4 or NV5. From a knowledge of the individual flow rates, the composition of the combined stream could be calculated. The e.m.f. output of the Wheatstone bridge was found to be a linear function of molar composition.

For calibrating the T/C cell with nitrogen-water vapor mixtures, the nitrogen gas was passed through the humidity control unit where it was conditioned to a known water vapor content. The gas stream then flowed directly to the T/C cell through the by-pass line provided at the three-way valve (TWV5 or TWV6). The calibration curves obtained are shown in Fig. 4 and 5. It can be seen that the water vapor content of a nitrogen stream can be very precisely determined using a T/C cell. That the calibration curve is not linear follows from the fact that the thermal conductivity of nitrogen-water vapor mixtures varies nonlinearly with composition (22).

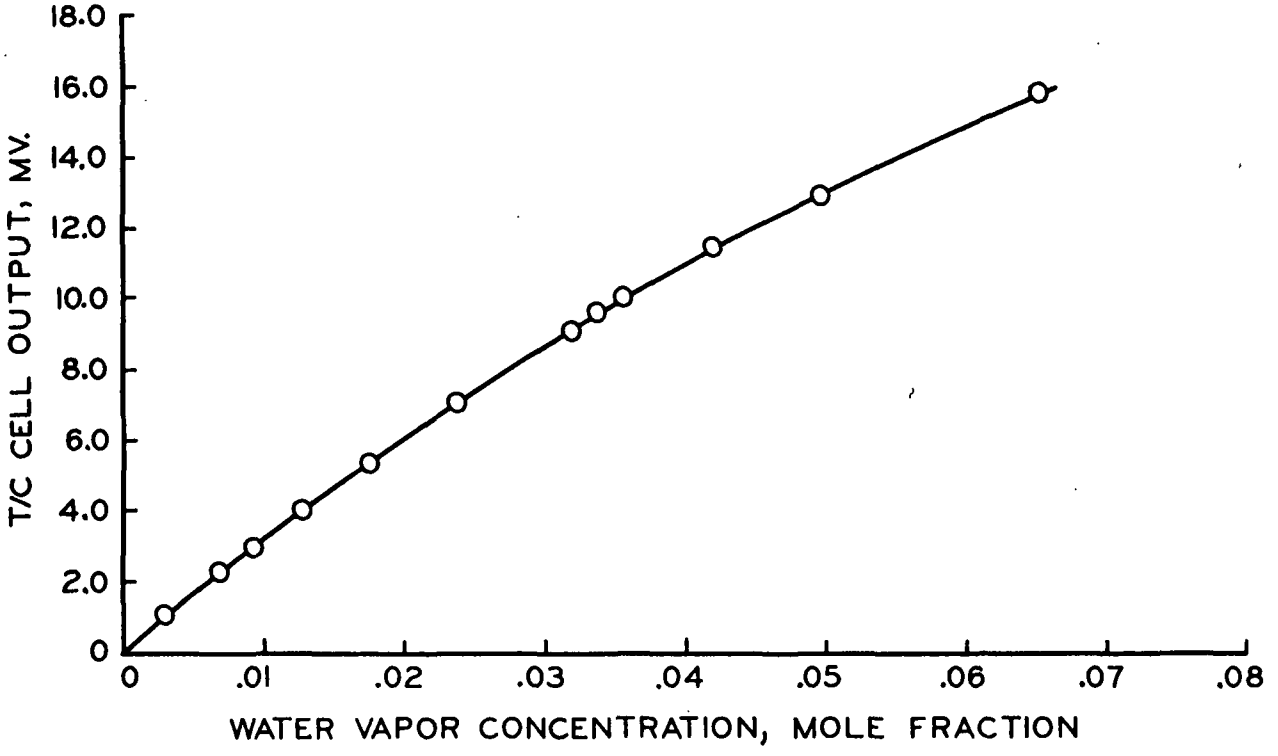

Figure 4. Calibration Curve for T/C 1: Water Vapor-Nitrogen at 40°C.

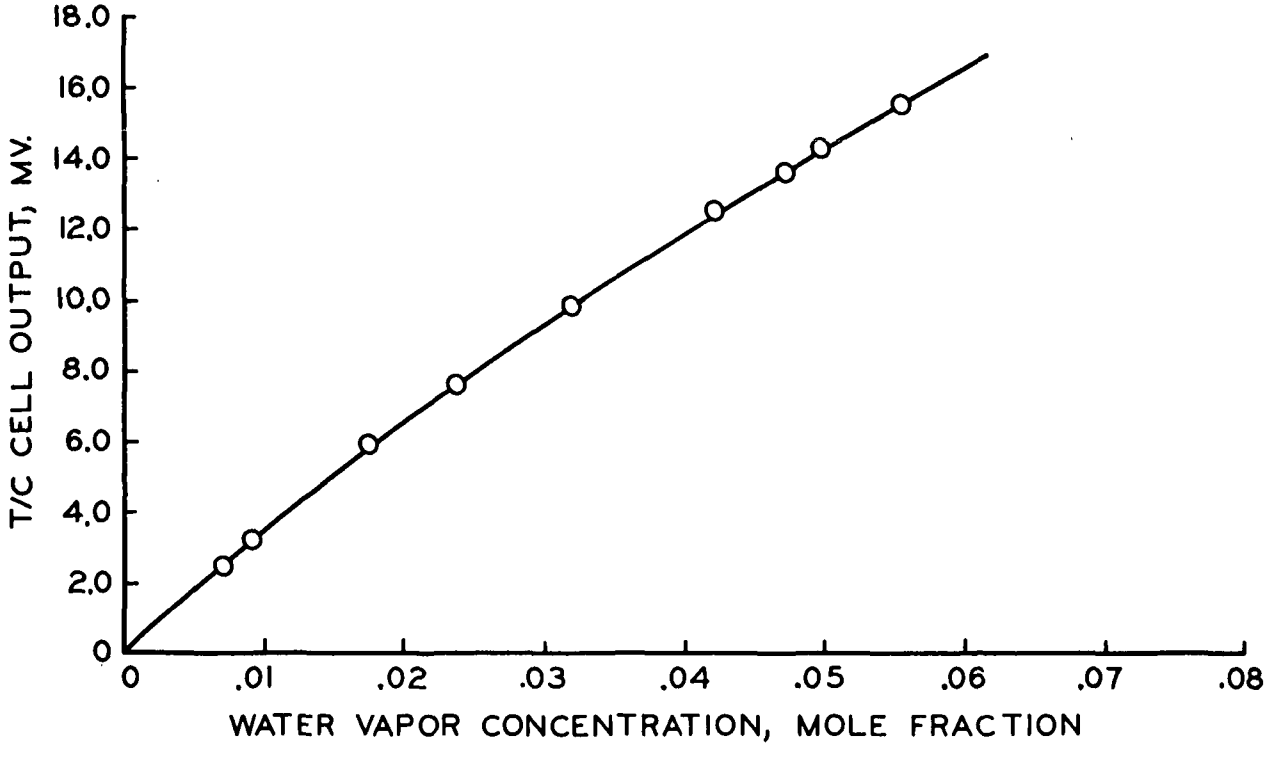

Figure 5. Calibration Curve for T/C 2: Water Vapor-Nitrogen at 40°C.

HUMIDITY CONTROL UNIT

The design for the humidity control unit was taken from Stafsing (23). A schematic drawing of the unit is shown in Fig. 6. A gas stream is first saturated with water vapor by passing through a gas dispersion tube (GDT) immersed in distilled water. The gas then passes through about 10 feet of 1/4-inch copper tubing immersed in a constant-temperature bath about 5°C. cooler than the first bath to condense excess moisture. The gas flows into a 1-1/2-inch copper pipe filled with glass wool to ensure that no water droplets are carried with the gas stream. As the stream emerges from the constant-temperature bath, the tubing is wrapped with heating wire to heat the stream and ensure that no further condensation takes place.

The system was checked by passing the humidified gas through weighed drying tubes containing calcium chloride and anhydrone. The wet-test meter measured the total dry gas flowing through the drying tubes. The amount of water adsorbed checked within 2% of the value calculated from the volume of dry gas and the vapor pressure of water at the temperature of the second bath. This difference was consistent and was probably the result of the drying tube not adsorbing all the water vapor.

OPERATING PROCEDURE

After a fiber mat, paper sheet, or polymer film had been placed in the diffusion chamber, it was assembled and the flow lines connected. The part of the flow system downstream from the flow control valves (Fig. 3, NV1 and NV2), excluding the micromanometer, was then slowly evacuated. If a pressure of at least 1 mm. Hg could not be attained, leaks were indicated. When the leaks had been eliminated, the evacuation was continued for about 18 hours. The temperature control elements of the air bath were activated and an overnight period of thermal equilibration was allowed.

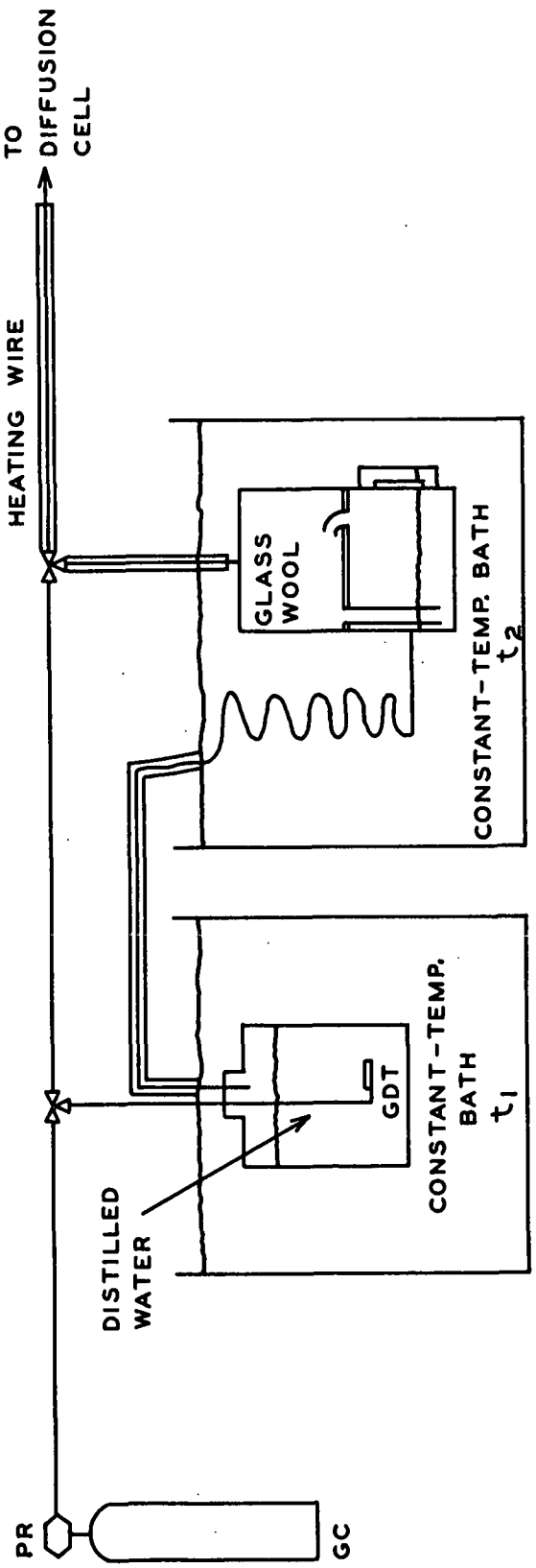

Figure 6. Humidity-Control Unit

The system was then slowly filled with the gases to be studied and the power supply to the T/C cells was turned on. A warm-up period of about four hours was allowed before the T/C cells were zero balanced. The T/C cells were zero balanced before and after every run to check any drift in the zero balance position. When water vapor and nitrogen were the two gases used, the calibration curve could also be checked quite easily by passing the nitrogen-water vapor stream directly to the sample passage of the T/C cell.

A diffusion run was started by opening toggle valves (TV1 and TV2), opening the three-way valves (TWV5 and TWV6) to the diffusion cell, and adjusting the inlet flows to approximately the same rate with needle valves NV1 and NV2. The recirculation pumps were then started. The scale reading of the micromanometer was noted when three-way valves TWV7 and TWV8 were open so that the two pressure taps to the micromanometer were directly connected. This scale reading was the "zero" position. The three-way valves (TWV7 and TWV8) were then opened so that the pressure difference between the two chambers of the diffusion cell could be measured. Needle valves NV4 and NV5 were adjusted to bring the micromanometer scale reading back to the "zero" position. This procedure was repeated throughout the course of an experiment.

Once stable flow rates and uniform total pressure were obtained, the bridge outputs of the T/C cells were recorded at regular intervals. When steady state was reached, the following data were recorded: barometric pressure, air bath temperature, diffusion chamber pressure, rotameter readings and pressures, and final T/C cell outputs. When the humidity control unit was used, the temperatures of the final water baths were recorded. Experiments with nitrogen and argon or carbon dioxide took only about one hour to reach equilibrium. After 24 hours, experiments with nitrogen and water vapor diffusing through thick wood pulp fiber mats were still approaching equilibrium. With paper sheets and polymer films, equilibrium was closely approximated

after six hours. From a material balance around the test section of the diffusion cell, the gas fluxes were calculated as shown in Appendix I.

MATERIALS TESTED

NYLON AND PULP FIBER BEDS

The nylon fiber mats used in preliminary studies were formed by constant-rate filtration of dilute fiber suspensions using equipment and techniques described by Bliesner (24) and Matters (15). Nylon fiber bed N-2 was formed with elliptical nylon 6 fibers. The average length of the fibers was 3.5 mm., the average width 100 μm., and the average thickness 20 μm. The elliptical fibers were used to form a fiber bed which could be compressed to a relatively low porosity when place in the diffusion cell. Several sulfite pulp fiber beds were also formed in the constant-rate filtration equipment. The beds formed in this apparatus had a diameter of 5 inches and when placed in the diffusion cell were compressed to a thickness of 1.191 cm.

PAPER SAMPLES

Paper samples S-1, S-2, and S-4 are bleached kraft papers obtained from Thilmany Pulp & Paper Company. Sample S-3 is a standard 42-lb. unbleached kraft linerboard. Physical data for these samples are given in Table II. The basis weight was determined for an oven-dried sample and the thickness was measured with a caliper gage which could be read to the nearest 0.02 mil (1 mil = 1/1000 inch). The thickness reported is the average of ten readings on a sample conditioned at room conditions. Thickness measurements were also made on samples which had been oven dried and on samples which had been conditioned at 75% relative humidity. The oven-dried samples usually had crinkled slightly and gave about the same thickness as the sample conditioned under room conditions. The increase in thickness at 75% R.H. was about 10%

over that determined at room conditions. Since the variation in thickness with relative humidity was small compared to changes in permeability and diffusion coefficients with increasing relative humidity, all calculations were based on the thicknesses measured at room conditions.

TABLE II

DATA ON PAPER SAMPLES

Sample	S-1	S-2 S-2.2	S-3	S-4 S-4.2
Basis weight, g./m.^{2}	45.7	40.2	184.5	51.9
Thickness, cm.	0.00663	0.00617	0.0338	0.00523
Apparent density, g./cc.	0.690	0.664	0.546	0.990
Mean pore diameter, μm. (Mercury intrusion)	1.3	2.3	--	0.25
Porosity, cc./cc. (Mercury intrusion)	0.352	0.425	--	0.272
Additives	None	None	None	None

The pore size distributions of paper Samples S-1, S-2, and S-4 were determined using a mercury intrusion porosimeter. The maximum in the volume-frequency curve for Sample S-1 occurred at an equivalent pore diameter of 1.3 μm. This is only about 10 times the mean free path of a nitrogen molecule at 40°C. and one atmosphere pressure. The use of the mercury porosimeter to determine pore size distribution on a compressible medium such as paper can be questioned. The results of studies with the mercury porosimeter are used only as part of the general description of the paper samples. Because the sample is compressed during mercury intrusion, the calculated pore diameters are probably smaller than the true pore diameters.

REGENERATED CELLULOSE FILM

The regenerated cellulose films used in this study were obtained from Bosites Machine Company. The film is used as a dialyzing membrane and had the designation 300 P.T. Cellophane. The cellophane (regenerated cellulose) contains about 20% glycerin to plasticize the sheet. Specimen R-1 was cut from an untreated dialyzing membrane and Specimen R-2 was cut from a cellophane film which had been leached for three days in fresh portions of distilled water to remove the glycerin. Other physical data on these samples are found in Table III.

TABLE III

DATA ON REGENERATED CELLULOSE AND CELLULOSE ACETATE FILMS

Sample	Description	Thickness, cm.	Density,[a] g./cc.
R-1	Plasticized regenerated cellulose film	0.00216	1.52
R-2	Leached regenerated cellulose film	0.00216	1.52
C-1	Solvent cast cellulose acetate film	0.00246	1.33

[a]Values taken from literature.

CELLULOSE ACETATE FILM

A cellulose acetate film was formed by casting an acetone solution of cellulose acetate on a clean mercury surface. The cellulose acetate was obtained in powder form from Eastman Chemical Products. Its designation was E 398-6 and Eastman reported that it had an acetyl content of 39.8% and a combined acetic acid content of 55.5%. Other physical data on the Sample (C-1) are given in Table III.

ADSORPTION ISOTHERMS

Water-vapor isotherms of the paper samples were determined using the method described by Wink (25). The specimen is placed in a holder which is suspended above different saturated salt solutions. When an equilibrium weight has been reached over one saturated salt solution, the specimen and specimen holder can be transferred to another beaker containing a different saturated salt solution. The salt solutions used in establishing the adsorption isotherm were LiCl, $MgCl_2$, KNO_2, NaCl, and $NH_4H_2PO_4$. The adsorption isotherms for paper Sample S-4 at 23°C. and 40°C. are given in Appendix II.

Many adsorption isotherms for regenerated cellulose (26-28) and cellulose acetate (26, 28, 29) are found in the literature. Since these are in quite good agreement, the values obtained by Jeffries (26) for regenerated cellulose and the values obtained by Newsome and Sheppard (29) for cellulose acetate were used in this study. These isotherms are given in Appendix II.

RESULTS AND DISCUSSION

From an overall material balance around the diffusion cell, one can calculate the fluxes through the barrier being tested for the particular conditions of that experiment. It is convenient to present the data by a proportionality factor or coefficient so that the results of each experiment are on a common basis. It will be assumed to start with that the counterdiffusion of two gases through the barrier is by normal diffusion and that Equation (10) is applicable. For true normal diffusion, the effective normal diffusion coefficient is inversely proportional to the total pressure, proportional to the three-halves power of the absolute temperature, and independent of the partial pressures. A general requirement of the diffusion cell is that all diffusion or permeability coefficients be independent of inlet flow rates. If the effective normal diffusion coefficient calculated using Equation (10) does not follow true normal diffusion behavior, the presence of complicating phenomena is indicated.

PRELIMINARY DIFFUSION EXPERIMENTS

In diffusion experiments using Matters' apparatus and investigating the counterdiffusion of nitrogen and argon through nylon fiber mats, it was noted that the effective normal diffusion coefficient calculated from Equation (10) was dependent on the inlet flow rates used, in contradiction to the results of Matters (15), who had found that within the precision of his data the effective normal diffusion coefficient was independent of the inlet flow rates he used. Since poor mixing of the inlet stream and the diffusing molecules at the mat surfaces could account for this behavior, two diaphragm pumps were placed in the system to recirculate part of the exit stream back to the inlet manifold ports. The pumps would lead to better mixing and higher sweep gas velocities without requiring greatly increased consumption of gases from the storage cylinders. The results of counterdiffusion experiments of

nitrogen and argon on nylon fiber bed N-2 (porosity = 0.664) are shown in Fig. 7. The effective normal diffusion coefficient attains a constant value only when the total flow rate to the test sections of the diffusion cell is about five times the flow rates Matters typically used during a run (10-20 millimoles/min. from each gas storage cylinder). Since Matters used nylon fiber beds of higher porosity (0.710 to 0.810), the effect of poor mixing at the bed surfaces is even more significant. It was estimated that as much as 50% of the diffusion resistance Matters measured might be due to poor mixing at the fiber bed surfaces.

The counterdiffusion of nitrogen and carbon dioxide through nylon fiber bed N-2 was studied to check Matters' suggestion that significant surface diffusion of carbon dioxide on nylon fibers occurred at sufficiently high pressures of carbon dioxide. The results for both nitrogen and argon and nitrogen and carbon dioxide counterdiffusion through nylon fiber mat N-2 are given in Table IV.

TABLE IV

EFFECTIVE NORMAL DIFFUSION COEFFICIENTS FOR NYLON FIBER BED N-2

Run No.	Gases	Temp., °C.	Flux Ratio, $\lvert \underline{r}_{\underline{\underline{AB}}} \rvert$	Total Pressure, atm.	$(\underline{\underline{D}}_{\underline{AB}})_{\underline{\underline{e}}} \underline{p}$, $cm.^2 sec.^{-1} atm.$	Diffusibility, δ
0314-1	N_2-A	40	1.28	0.982	0.0346	0.159
03125-1	N_2-CO_2	40	1.34	0.975	0.0288	0.161
03126-1	N_2-CO_2	40	1.26	0.978	0.0289	0.161

In contrast to Matters' results, the flux ratio for nitrogen and carbon dioxide counterdiffusing through a nylon fiber bed was within experimental error of the expected value for normal diffusion of $(\underline{M}_{CO_2}/\underline{M}_{N_2})^{1/2} = 1.25$ even at a total pressure of 1 atm. Matters found that, as he increased the total pressure in his experiments, the flux ratio, $\lvert \underline{N}_{N_2}/\underline{N}_{CO_2} \rvert$, decreased from a value of 1.2 at 0.2 atm. total pressure

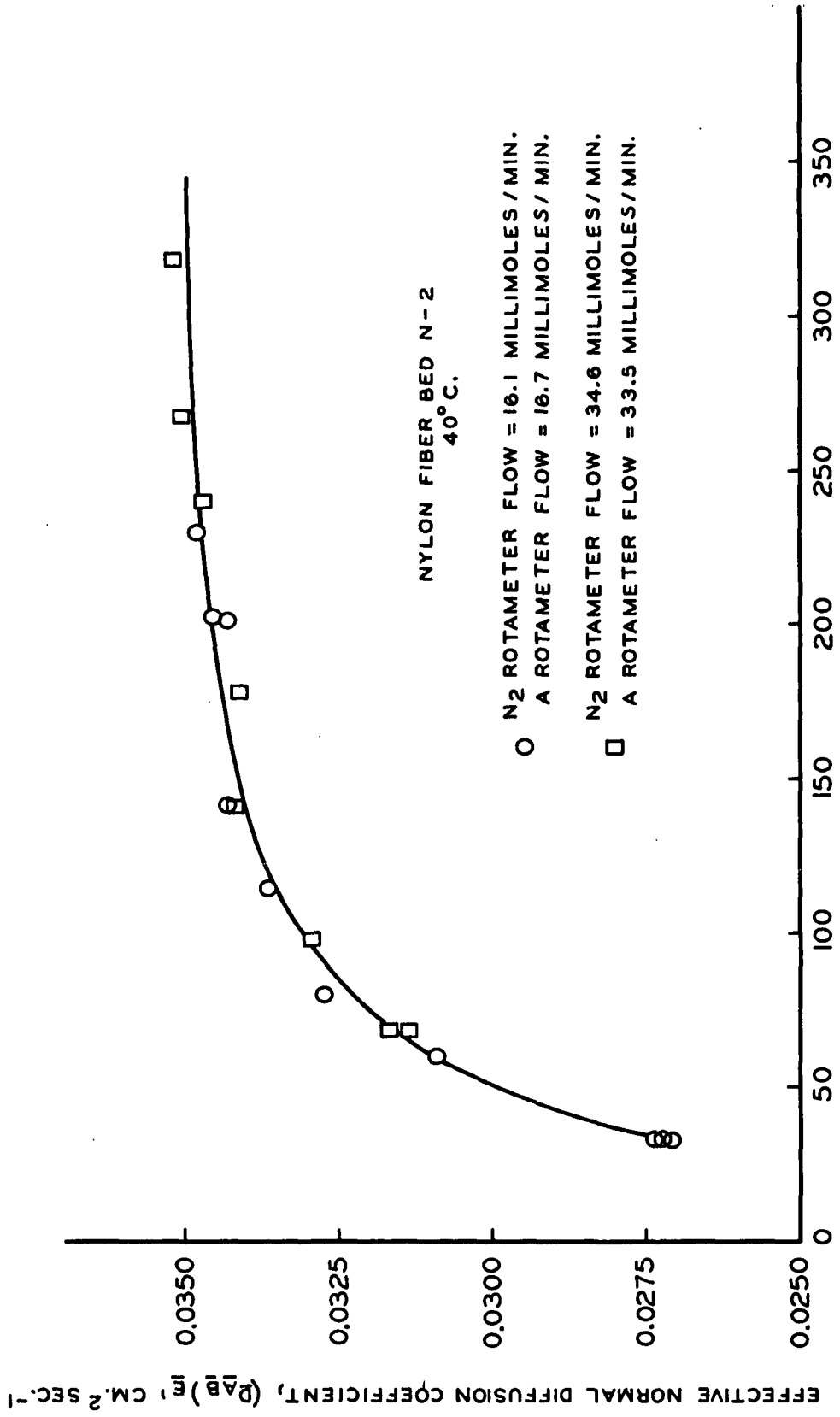

Figure 7. Effect of Increasing Flow Rates to Inlet Manifold Ports

to a value of 0.7 at 1 atm. total pressure. He attributed this to augmented flux of adsorbed carbon dioxide due to surface diffusion. The present results show that nitrogen and carbon dioxide diffuse through nylon fiber mats in a normal manner. A further check on the internal consistency of the present results is given by the close agreement in the value of the diffusibility calculated for a nitrogen-argon experiment to those for the nitrogen-carbon dioxide experiments. That the variation in the flux ratio found by Matters was not due to poor mixing at the fiber bed surfaces is known from the results of the experiments given in Fig. 7. For all 19 experiments the flux ratio, $|\underline{N}_{N_2}/\underline{N}_A|$, was independent of flow rate and had values between 1.22 and 1.35; the ratio $(\underline{M}_A/\underline{M}_{N_2})^{1/2}$ equals 1.17.

Matters' results were probably caused by an operating procedure which gave rise to increasing total pressure differences across the fiber mat as the total pressure was increased. The diffusion cell and pressure lines were evacuated before each series of runs. Then nitrogen and carbon dioxide were introduced slowly into the respective half-cells of the diffusion chamber until the desired pressure was reached. The pressure control system was activated, the inlet flow rates were adjusted to their final values, and the pressures were balanced to bring the meniscuses of the inclined manometers to the "zero balance" position determined under vacuum. This method of filling the diffusion cell results in the pressure lines to the inclined manometers being filled with gas rich in either nitrogen or carbon dioxide. Because of differences in the densities of the gases in the pressure lines, a difference in height between the level of the manometer fluid and the average level of the pressure taps could result in a true "zero balance" position different than the "zero balance" position under high vacuum. Assuming that the pressure lines to the top half-cell were filled with nitrogen and that the lines to the bottom half-cell were filled with carbon dioxide, the location of the inclined manometer for balancing the top and bottom test sections of the diffusion cell would result in a pressure imbalance of about 5 dynes/cm.^{2} at a total

pressure of one atmosphere. Matters found significant forced flow at these low total pressure differences.

Preliminary experiments counterdiffusing nitrogen and water vapor through nylon fiber and wood pulp fiber beds showed that within the precision of the data the results could be explained in terms of the ordinary counterdiffusion of two gases. It appeared that in these porous structures gas-phase diffusion predominated and there was no evidence of diffusion in the sorbed phase.

DIFFUSION THROUGH PAPER SAMPLES

The effective normal diffusion coefficients for nitrogen and argon diffusing through paper Samples S-1 and S-2 were determined. The results are given in Table V.

TABLE V

EFFECTIVE NORMAL DIFFUSION COEFFICIENTS FOR PAPER SAMPLES S-1 AND S-2

Run No.	Sample	Gases	Flux Ratio, $\lvert \underline{\underline{r}}_{AB} \rvert$	Total Pressure, atm.	$(\underline{\underline{D}}_{AB})_e \underline{p} \times 10^4$, $cm.^2 sec.^{-1} atm.$	Temp., °C.
0610-1	S-1	N_2-A	1.34	0.975	0.645	40
0611-1	S-1	N_2-A	1.36	0.975	0.651	40
0611-2	S-1	N_2-A	1.32	0.968	0.656	40
0618-2	S-2	N_2-A	1.18	0.995	9.68	40
0618-3	S-2	N_2-A	1.21	0.992	9.48	40

The effect of sweep gas velocity on the value of the effective normal diffusion coefficient was checked. If the diaphragm pumps were not used to recirculate part of the exit streams, the calculated diffusion coefficients were about 15% lower than those reported in Table V. As the amount of gas recirculated increased, the coefficient increased asymptotically to the value given in Table V. When the rate of

recirculation was three times the fresh gas flow rate, the value of the diffusion coefficient was no longer dependent on recirculation rate. All further experiments were carried out with a recirculation rate of five times the fresh gas flow rates.

All diffusion experiments were made at pressures of about 1 atm. Since the normal diffusion coefficient is inversely proportional to total pressure and the Knudsen diffusion coefficient is independent of total pressure, such experiments would indicate the controlling mechanism in gas-phase diffusion. The mercury porosimeter measurements showed that the maximum in the volume-frequency curve for Sample S-1 occurred at an equivalent pore diameter of 1.3 μm. Since this diameter is about ten times the mean free path of a nitrogen molecule at 40°C. and 1 atm., it was assumed that the normal diffusion equation best described the diffusion process. If the molecular weights of two gases used in counterdiffusion studies are equal, the flux ratio is equal to one and the equations for normal and Knudsen diffusion are the same for this special case. If the flux ratio is different from one, the value of the effective diffusion coefficient calculated from Equation (11) will be different from that calculated using Equation (10), depending on the magnitude of the flux ratio. Since for nitrogen and argon the flux ratio is fairly close to one, the effective diffusion coefficient calculated by either equation will differ from the other by less than 5%.

Counterdiffusion experiments with nitrogen and argon in the presence of a fixed concentration of water vapor were made on paper Sample S-1. The purpose of this was to determine if the sorption of water vapor and accompanying swelling would affect gas-phase diffusion through the sample. Two experiments were made: one at a concentration of water vapor corresponding to 32% relative humidity and the other at 63% R.H. The results are given in Table VI. Because the partial pressure of water vapor was the same at both faces of the sample, there was no net flux of water vapor through the sample.

TABLE VI

EFFECT OF RELATIVE HUMIDITY ON GAS-PHASE DIFFUSION FOR SAMPLE S-1

Run No.	Temp., °C.	Gases	Flux Ratio, $\lvert \underline{\underline{r}}_{AB} \rvert$	Total Pressure, atm.	$(\underline{\underline{D}}_{AB})_e \underline{\underline{p}} \times 10^4$, $cm.^2 sec.^{-1} atm.$	R.H., %
0617-1	40	N_2-A	1.60	0.990	0.56	32.0
0617-2	40	N_2-A	1.50	0.980	0.55	63.2

For these experiments, both the argon and the nitrogen streams were passed through the humidity control unit and conditioned to the same moisture content. Thermal conductivity cell calibration curves could be obtained, and the effective normal coefficients were calculated using Equation (10). In general, the diffusion coefficients for a tertiary gas mixture are different from the binary diffusion coefficient. Because the concentration of water vapor is quite low (< 6%), one might expect that its presence would not materially affect the binary normal diffusion coefficient of nitrogen and argon. Comparison of the effective normal diffusion coefficients for Sample S-1 given in Tables V and VI shows that the presence of water vapor does not greatly change the calculated diffusion coefficient. The T/C cell calibration curves for these experiments were drawn from very few calibration points and hence the experimental errors in the determination of exit stream composition could have been quite large.

The counterdiffusion of nitrogen and water vapor through paper Samples S-1, S-2, S-3, and S-4 was studied. Because very small partial pressure differences of nitrogen and water vapor were maintained across the sample, the fluxes of nitrogen and water vapor were correspondingly small. These fluxes were so small relative to the flow rates of the incoming gas streams that the calculation of the fluxes and the flux ratio from an overall material balance around the diffusion cell became very sensitive to experimental errors in flow rate and composition determinations. The equations for

the fluxes of water vapor and nitrogen calculated from an overall material balance include all the flow rate and composition determinations obtained in the experiment. When the mole fractions are very large or very small, the differences in these equations are small relative to the numbers being subtracted and the effect of experimental error on the calculation is large. If it is assumed that the difference between the fluxes of nitrogen and water vapor is small compared to the total inlet gas flow rates, the equations become much simpler. Two independent calculations of the water-vapor flux can be made from material balances around the top and the bottom halves of the diffusion cell. These calculations usually agreed within 10%.

Since the flux ratios for nitrogen-water vapor experiments could not be determined with any precision, it was assumed for the purposes of calculating an effective normal diffusion coefficient that the flux ratio was given by $(M_{H_2O}/M_{N_2})^{1/2} = 0.802$. The results of such calculations for experiments with Samples S-1, S-2, S-2.2, and S-4 are given in Fig. 8. The effective normal diffusion coefficients are correlated with the relative humidity at which the experiments were carried out. The range of the segments used to represent a single diffusion experiment give the relative humidities of the exit streams from the two test chambers of the diffusion cell. These relative humidities represent the partial pressures of water vapor at the surfaces of the sample during the diffusion run. Because of the dependence of the diffusion coefficient on mean partial pressure of water vapor, it is clear that the normal diffusion equation does not account for the observed behavior. It is interesting to note, however, that if the diffusibility calculated from nitrogen-argon counterdiffusion experiments is used to calculate an effective normal diffusion coefficient for nitrogen and water vapor through the same sample that this coefficient coincides with the extrapolation to zero relative humidity of the experimentally determined nitrogen-water vapor diffusion coefficients. It appears that at low relative humidities the transport of water vapor through paper takes place only in the gas phase. Effective

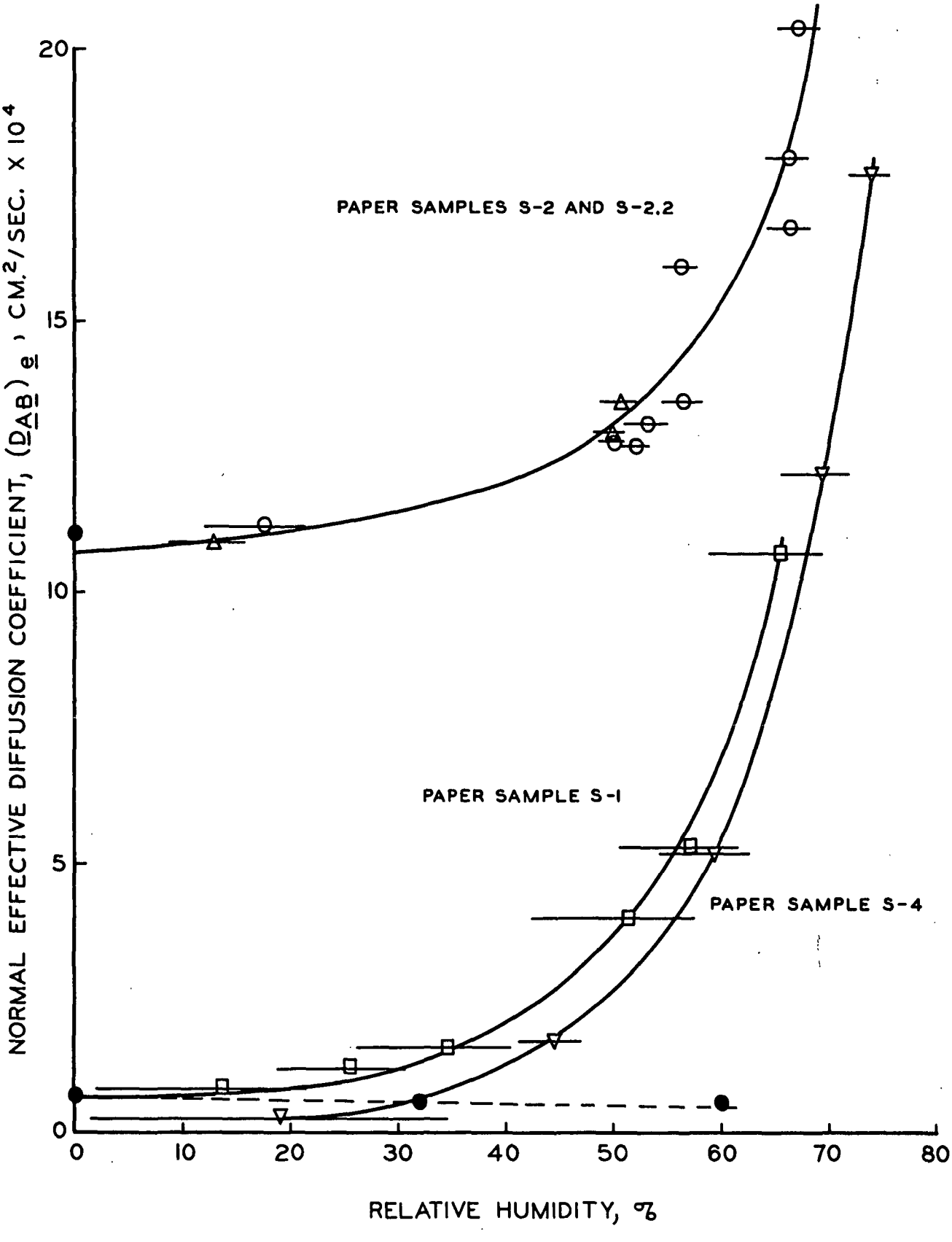

Figure 8. The Effect of Relative Vapor Pressure on Effective Normal Diffusion Coefficient

normal diffusion coefficients calculated from the results of the nitrogen-argon-water vapor experiments on Sample S-1 are included in Fig. 8 (dashed line) to show that the presence of water vapor does not greatly affect the counterdiffusion in the gas phase.

To insure that the dependence of the nitrogen-water vapor diffusion coefficients on water-vapor pressure was not an artifact of the equipment or operating procedure, the diffusion runs were made in mixed order. In some experiments the water-vapor concentration was higher in the top stream and in others the reverse was true. A series of diffusion runs included runs made at a mean vapor pressure lower than the previous experiment as well as runs at a mean vapor pressure higher than the previous experiment. The same dependence of the effective normal diffusion coefficient on relative humidity was observed for the kraft linerboard sample (S-3). The diffusion coefficients for Sample S-3 were not included in Fig. 8 because they were much higher than for the more dense papers (58.6×10^{-4} cm.^{2} sec.$^{-1}$ at 16% R.H. and 65.9×10^{-4} cm.^{2} sec.$^{-1}$ at 60% R.H.).

Since the diffusion coefficient calculated from a given experiment is determined for a finite range of relative vapor pressures, the diffusion coefficient at any particular vapor pressure can be determined by the method of successive approximations. This is done graphically by drawing the smoothed-data curve so that the areas above and below the segment representing a single diffusion experiment and bounded by the smoothed-data curve are approximately equal. For a parabolic function, the data points are located by $RH = \sqrt{(RH2^2 + (RH2)(RH1) + RH1^2)/3}$ where RH1 and RH2 are the low and high values over the interval, respectively. The smoothed-data curves were drawn through the points located in this manner.

The gaseous transport of water vapor through paper Samples S-1, S-2, S-3, and S-4 is clearly being augmented by sorbed vapor transport at the higher relative

humidities. A sorbed vapor permeability coefficient, P_s, can be defined which does not assume any particular mechanism of sorbed vapor transport:

$$P_s = N_{As}/[(p_{A_2} - p_{A_1})/L] \qquad (16)$$

where $(p_{A_2} - p_{A_1})$ is the partial pressure difference of water vapor across the sample and N_{As} is the sorbed vapor flux.

The temperature dependence of sorbed water transport was investigated for Sample S-4 because of the insignificant amount of gas-phase transport through the sample. The results at 30, 40, and 50°C. are given in Fig. 9. The sorbed vapor-permeability coefficient increases rapidly with increasing relative pressure but is apparently independent of temperature for a given relative humidity over the range studied. This is in contrast to Scheschels (30) who found that the sorbed vapor-permeability coefficient for paper decreased more than 40% at a given relative humidity when the temperature was increased from 20 to 70°C. The present results are supported by Stannett, et al. (31) and Barrer (32) who state that the water-vapor permeability coefficients of most cellulosic films appear to be independent of temperature in this range.

DIFFUSION THROUGH REGENERATED CELLULOSE FILMS

A regenerated cellulose film was studied to compare the water-vapor transport through paper to that of a cellulosic material without the extensive fiber surface area or the inter- and intrafiber capillary structure of a paper sheet. Since the permeability coefficient of a regenerated cellulose film to nitrogen is extremely small [$P_{N_2} \simeq 1 \times 10^{-20}$ (moles cm.)/(sec. dynes)], only nitrogen-water vapor studies were made. The sorbed vapor permeability coefficients for the plasticized (R-1) and leached (R-2) cellophane films are given in Fig. 10. The sorbed vapor permeability

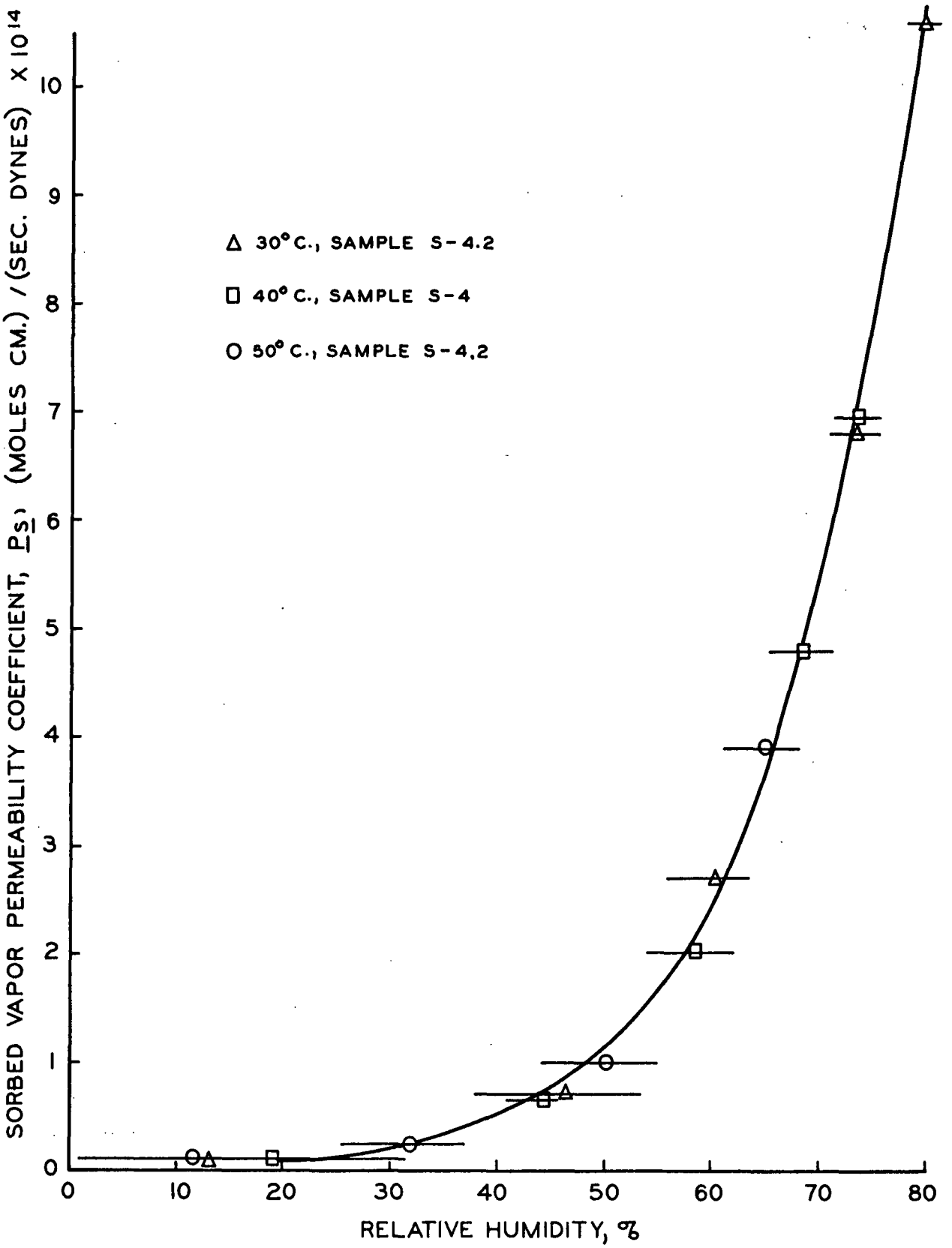

Figure 9. Sorbed Vapor Permeability Coefficients for Paper Sample S-4

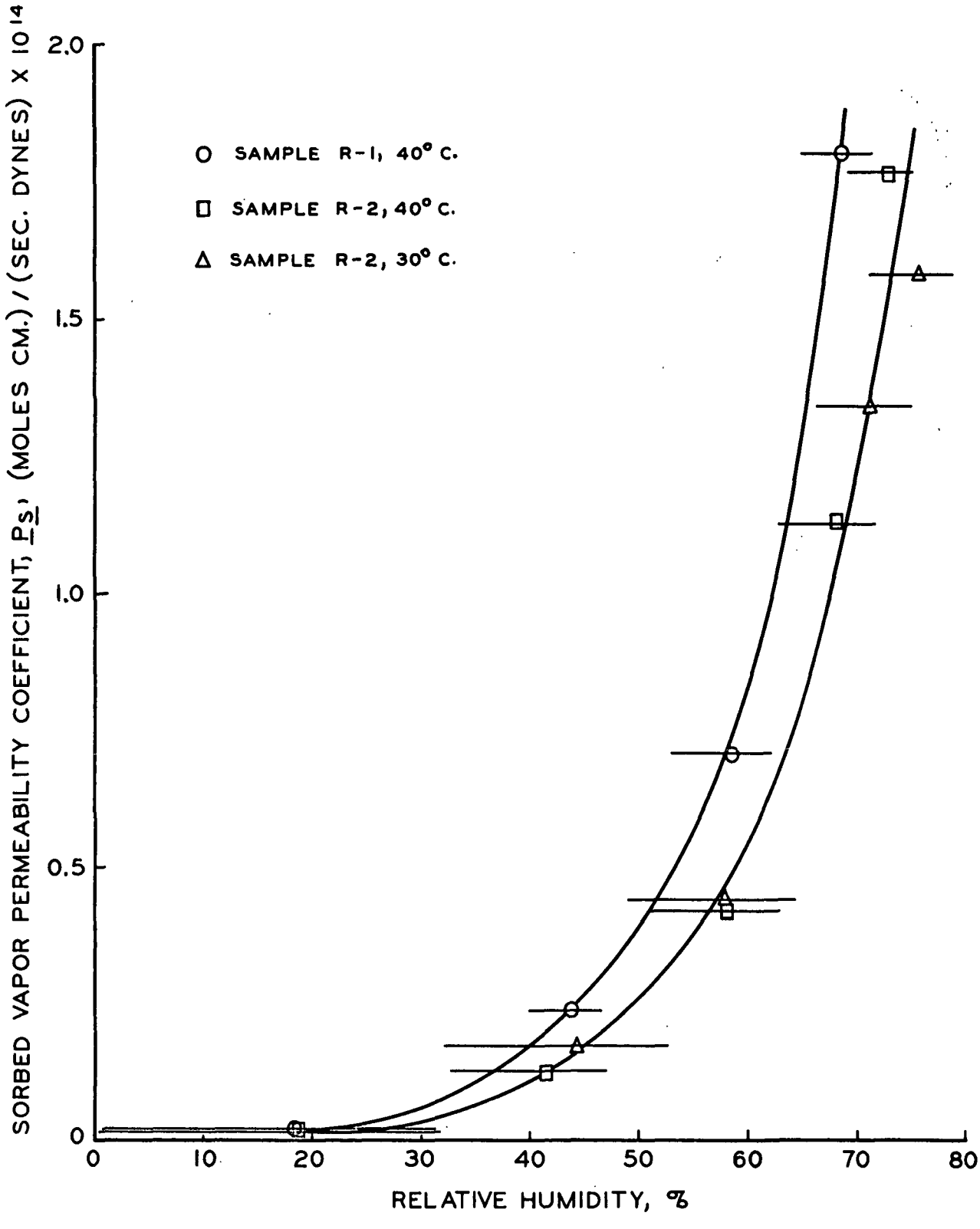

Figure 10. Sorbed Vapor Permeability Coefficients for Regenerated Cellulose Films

coefficient increases with increasing relative humidity in exactly the same manner as the coefficient for a paper sample. The difference in magnitude ($\underline{P}_s$ for Sample S-4 is about four times $\underline{P}_s$ for Sample R-2 at any given relative humidity) of the coefficients can be explained in terms of the void structure of the paper sheet. The gas-phase flux through the continuous pores of the medium has already been accounted for, but the flux of water vapor through paper in the sorbed phase is likely to be a combination of gas-phase diffusion through voids and sorbed-phase diffusion through the solid phase. The sorbed vapor flux is controlled by diffusion in the solid phase, but the magnitude of the coefficient is higher in paper than in regenerated cellulose because part of the diffusion path is through the voids of the paper.

The permeability coefficient for the plasticized cellophane film increased more rapidly with increasing relative humidity than for the sample which was leached with water. At any given relative humidity, this difference was about 40%. The permeability coefficient for Sample R-2 was determined at 30 and 40°C., and within experimental error there is no temperature dependence if the permeability coefficient is plotted versus relative humidity.

DIFFUSION THROUGH CELLULOSE ACETATE FILM

The sorbed vapor-permeability coefficients for paper and regenerated cellulose have approximately the same dependence on relative vapor pressure. This indicated that fiber surface area and intrafiber pores were not significant in the sorbed vapor transport. Since both media have an abundance of hydroxyl groups and strong hydrogen bonding between cellulose polymer chains, it would be interesting to note the effect of introducing bulky substituent groups to a cellulosic medium. The cellulose acetate film studied had on the average about 2.5 acetyl groups per anhydroglucose monomer unit. The presence of the acetyl groups on cellulose affects the packing

of the polymer chains and in general leads to a less strongly hydrogen-bonded system. The cellulose acetate film is hydrophilic, as evidenced by its strong adsorption of water vapor.

The permeability of a cellulose acetate film to a permanent gas such as nitrogen [$P_{N_2} \simeq 1 \times 10^{-18}$ (moles cm.)/(sec. dynes)] is much lower than for water vapor but higher than the permeability of a regenerated cellulose film to nitrogen. The results of diffusion studies on the cellulose acetate film (C-1) are presented in Fig. 11. The sorbed vapor permeability coefficient for water vapor is much higher at low relative humidities for cellulose acetate than for either paper or regenerated cellulose. The permeability coefficient increases with increasing relative humidity for the cellulose acetate film, but this increase is not nearly as rapid as for paper or regenerated cellulose. At 70% R.H., the permeability coefficient for regenerated cellulose is higher than for cellulose acetate. Hauser and McLaren (33) reported similar findings. Wellons (34) studied the water-vapor permeation of a solvent-cast cellulose acetate film and reported permeability coefficients of the same magnitude and with the same dependence on relative humidity as those given in Fig. 11. Wellons calculated his permeability coefficients as integral values, meaning the average permeability coefficient between zero and some given relative humidity. If his data are recalculated to determine differential or point values of the permeability coefficient, his data fit the curve in Fig. 11 very well.

DIFFUSION COEFFICIENTS FOR SORBED VAPOR TRANSPORT

As indicated earlier, the thermodynamic driving force for diffusion is the chemical potential. For the gases and vapor used, the fugacity or activity coefficient is different from one only at pressures much higher than one atmosphere. Thus, Fick's first law is an appropriate starting equation when analyzing gas-phase diffusion.

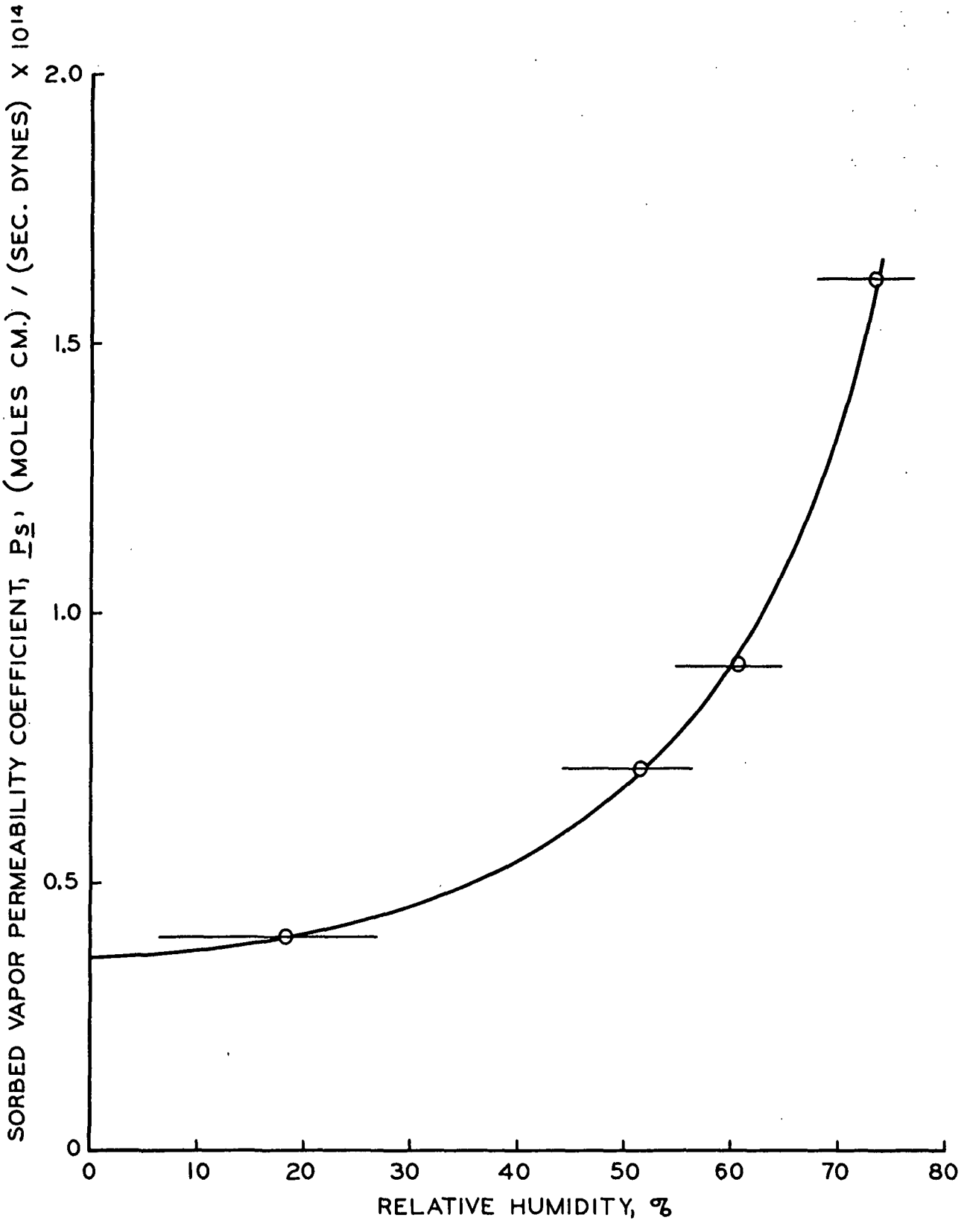

Figure 11. Sorbed Vapor Permeability Coefficient for Cellulose Acetate Film at 40°C.

For gas or vapor molecules dissolved in a liquid or solid, the concentration-vapor pressure curve is often linear in the low concentration range and Henry's law is said to be obeyed. Over the range in which Henry's law is obeyed, the activity coefficient is a constant and Fick's law is again an appropriate starting equation. It is clear from the water-vapor adsorption isotherms for paper, regenerated cellulose, and cellulose acetate given in Appendix II that these systems are far from ideal. For paper and regenerated cellulose, Henry's law does not hold even at the lowest concentrations.

To treat the nonideal case, it will be necessary to define the activity and activity coefficient further. The first part of the definition of the activity is given by

$$\mu = \mu_* + RT \ln a \tag{17}$$

where μ_* is a standard chemical potential. Before any numerical values can be assigned to the activity, some kind of reference function must be assumed and some particular state must be chosen in which the activity approaches or equals the value of the reference function. It will be convenient for our purposes to assume for the second part of the definition of the activity that

$$\lim_{c_s \to 0} \frac{a}{c_s} \to 1. \tag{18}$$

The activity coefficient is given by

$$\gamma = \frac{a}{c_s} . \tag{19}$$

The chemical potential of the gas or vapor in the gaseous phase, assumed to be ideal, is given by

$$\mu = \mu^* + RT \ln p_A \tag{20}$$

where μ^* is a chemical potential in a standard state. At equilibrium, the chemical potential of any species must be the same in both the sorbed and gas phases. Therefore,

$$\mu_* + RT \ln a = \mu^* + RT \ln p_A \qquad (21)$$

By rearrangement

$$\mu_* - \mu^* = RT \ln \frac{p_A}{a} = RT \ln K \qquad (22)$$

where K is the equilibrium constant given by the slope of the adsorption isotherm at $c_s = 0$. Rearranging gives

$$K = \exp[(\mu_* - \mu^*)/RT] \qquad (23)$$

or

$$p_A = Ka \; . \qquad (24)$$

The diffusion equation based on activity can now be written in terms of measurable variables. Rewriting Equation (7), we have

$$\vec{N}_{As} = D_s c_s \frac{d(\ln a)}{dz} = D_s \frac{c_s}{a} \frac{da}{dz} \; . \qquad (25)$$

Substituting for a, one obtains

$$\vec{N}_{As} = D_s \frac{c_s}{p_A} \frac{dp_A}{dz} \; . \qquad (26)$$

Noting that $\vec{N}_{As}/(dp_A/dz)$ is the sorbed vapor permeability coefficient,

$$D_s = \frac{p_A}{c_s} P_s \; . \qquad (27)$$

If Fick's first law is assumed, the equation is

$$\vec{N}_{As} = D_{sf} \frac{dc_s}{dz} = D_{sf} \frac{dc_s}{dp_A} \frac{dp_A}{dz} \qquad (28)$$

or

$$D_{sf} = \frac{dp_A}{dc_s} P_s \quad . \qquad (29)$$

where D_{sf} is the Fick's law diffusion coefficient. The diffusion coefficients calculated from Equations (27) and (29), the adsorption isotherms, and smoothed values of P_s are given in Fig. 12, 13, and 14 as a function of sorbed vapor concentration for Samples S-4, R-1, and C-1. The diffusion coefficients based on chemical potential as the driving force for diffusion appear to be more simply related to the concentration than the diffusion coefficients based on concentration as a driving force. Both, however, are strongly dependent on concentration.

If at a given concentration the logarithms of the diffusion coefficients calculated for Sample S-4 from the general diffusion equation are plotted against the inverse of the absolute temperature, a series of nearly parallel straight lines results (Fig. 15). The temperature dependence of the diffusion coefficient of a gas diffusing through a polymer is usually given by (2).

$$D_s = D_{s_o} \exp(-\Delta E_D/RT) \qquad (30)$$

where ΔE_D is the activation energy for diffusion and D_{s_o} is a theoretical diffusion coefficient at infinite temperature. The Arrhenius-type temperature dependence is quite general for any process that involves an activated state. The activation energy for diffusion from the slopes of the lines in Fig. 15 is approximately 13 kcal./mole. This value is close to the activation energies of diffusion coefficients for most gas-polymer systems and lies within the range of values for the water-vapor permeation of polyethyl methacrylate reported by Stannett and Williams (35).

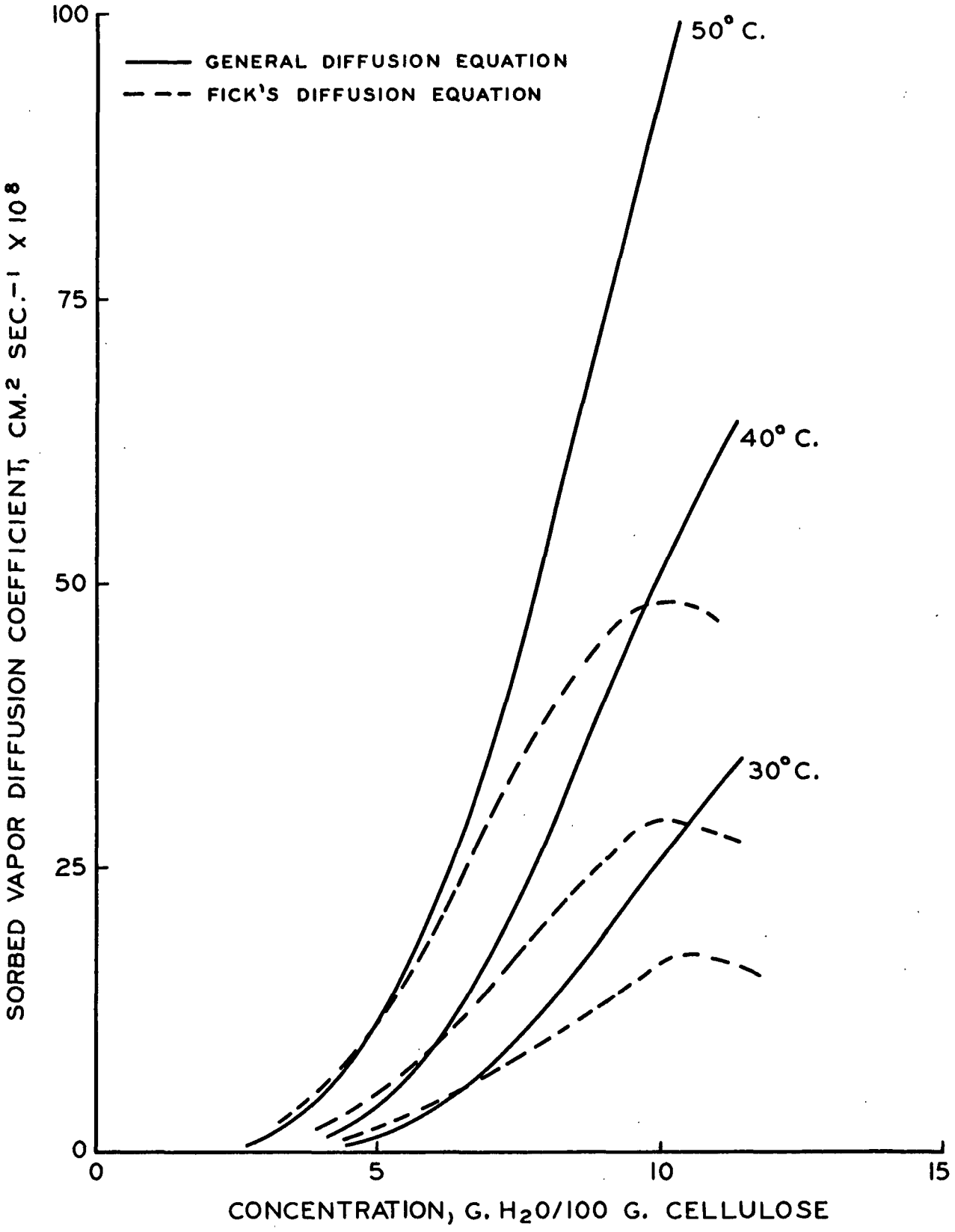

Figure 12. Sorbed Vapor Diffusion Coefficients for Paper Sample S-4

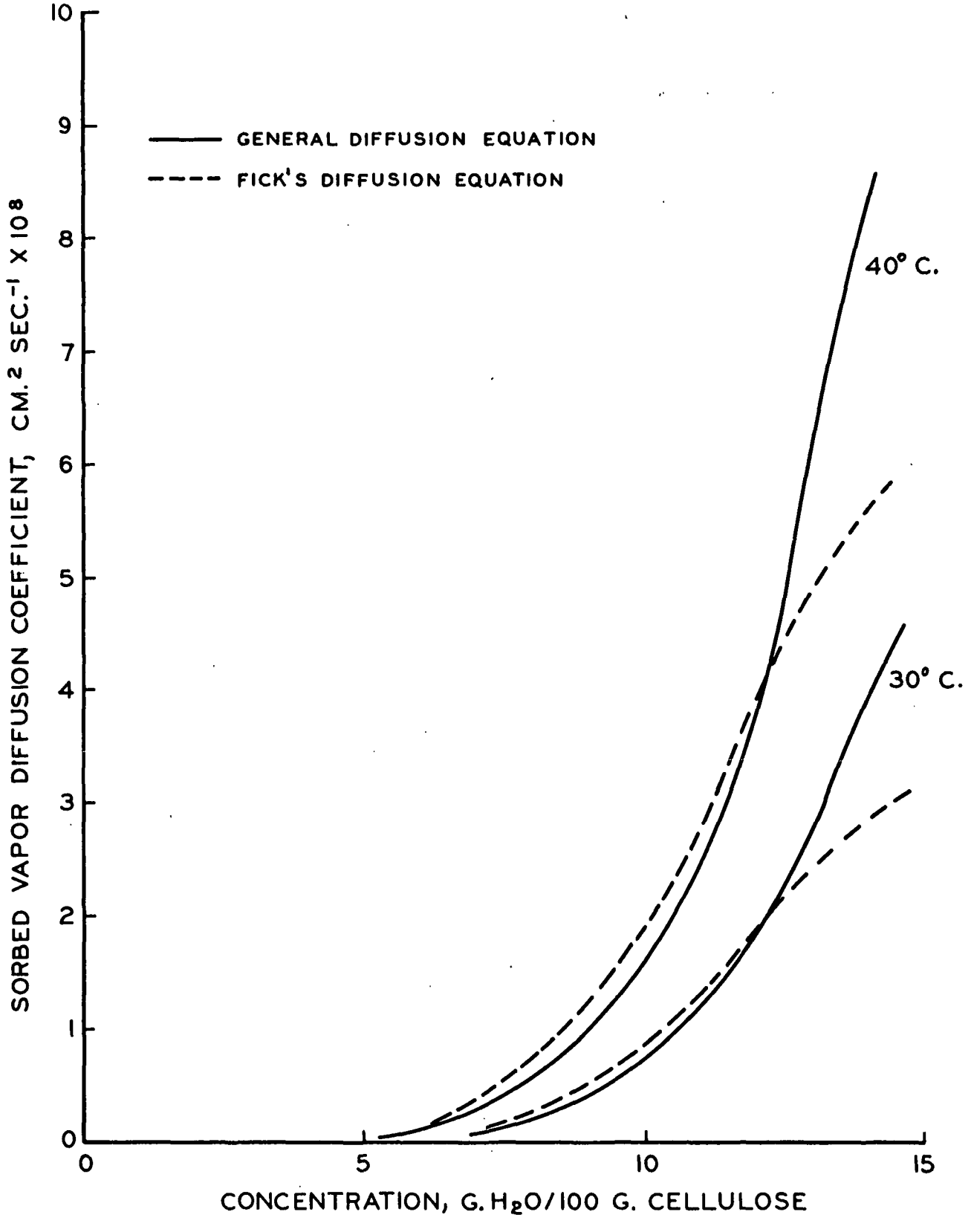

Figure 13. Sorbed Vapor Diffusion Coefficients for Regenerated Cellulose Sample R-2

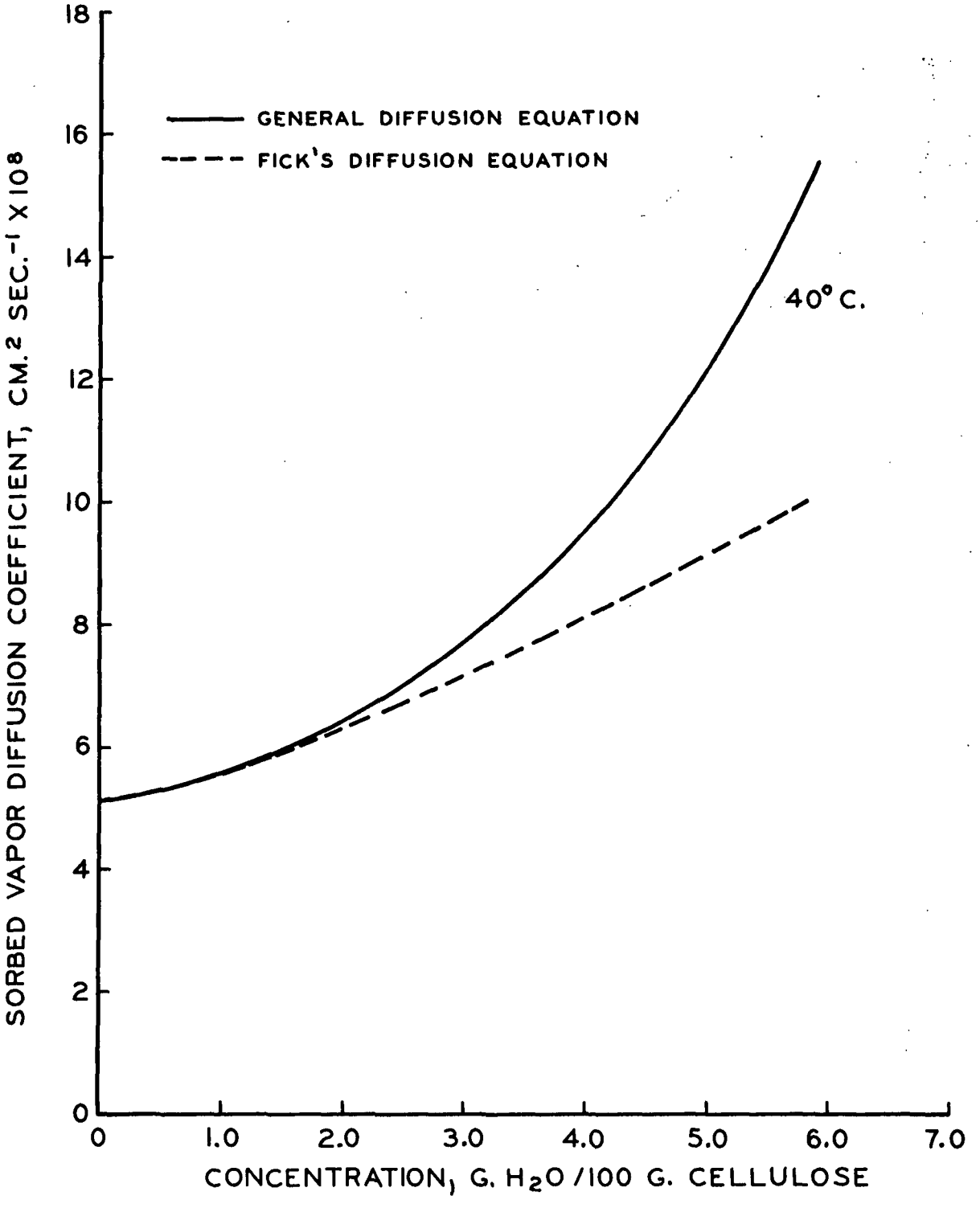

Figure 14. Sorbed Vapor Diffusion Coefficients for Cellulose Acetate Sample C-1

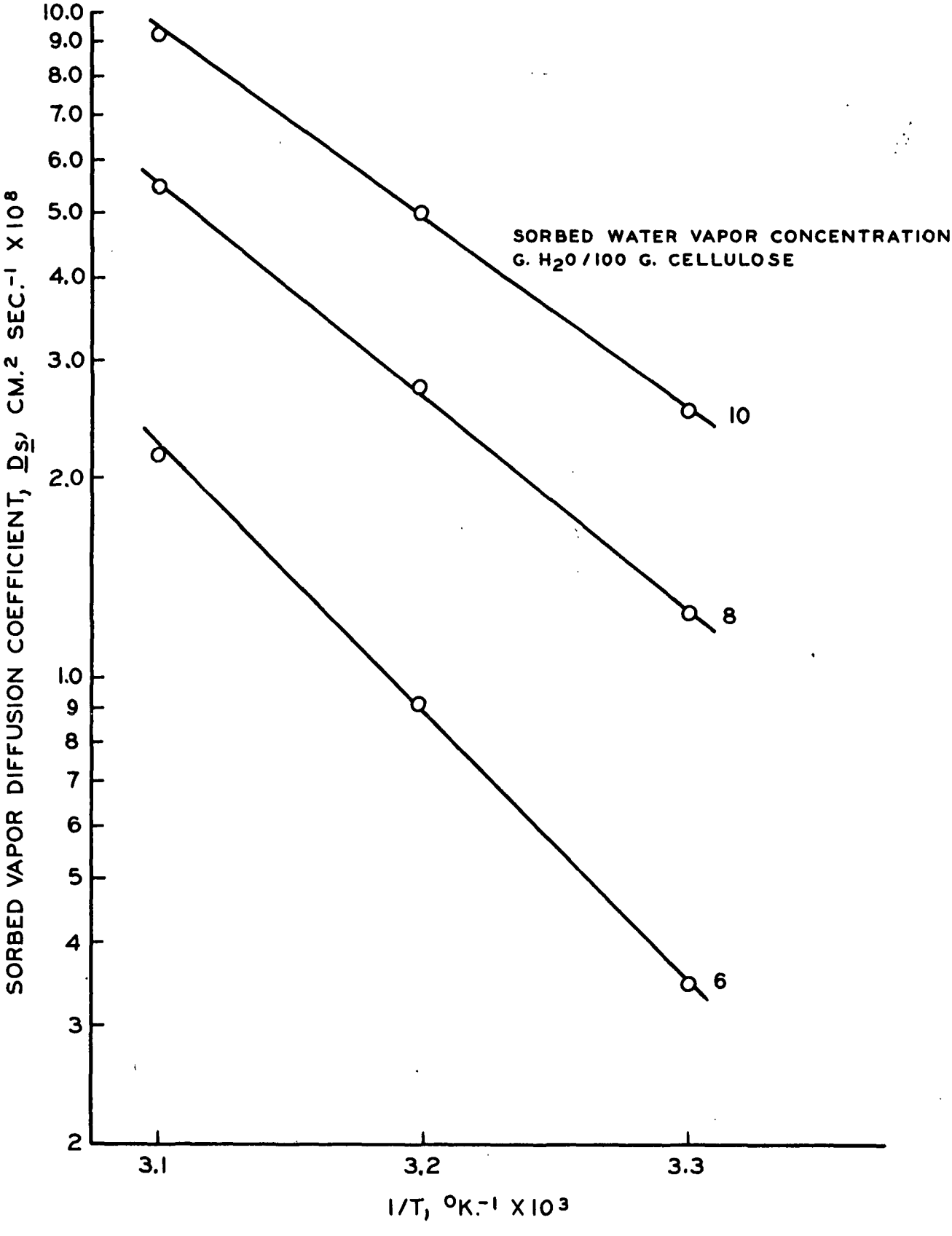

Figure 15. Effect of Temperature on General Sorbed Vapor Diffusion Coefficient for Sample S-4

ANALYSIS OF RESULTS

Each of the possible mechanisms which could account for the sorbed water transport are analyzed to see which model best accounts for the results of the present and previous investigations. It is, of course, quite probable that capillary condensed flow, surface diffusion, and solid solution diffusion all contribute somewhat to the sorbed water transport through cellulosic materials.

CAPILLARY CONDENSED FLOW

A number of early investigators considered that the adsorption of water vapor by cellulose was by capillary condensation after the initial adsorption on exposed adsorption sites. Thus, the adsorption isotherm for cellulose above a relative pressure of 0.20 could be explained by vapor condensation in capillaries of increasing diameter. It is difficult to reconcile the great specificity of water-vapor sorption by cellulose with the very small adsorption of benzene at the same relative pressure of each sorbate according to the capillary theory (36). The capillary theory offers no explanation for the swelling which always accompanies water-vapor sorption or for the fact that many fibers or films such as those from regenerated cellulose do not have any permanent capillary space (37). Capillary condensation can be considered to be the take-up of water in transient capillaries or spaces that exist only in the presence of water. The take-up of water in such structures does not involve the replacement of a solid-air or solid-vacuum interface with a solid-liquid interface as is the case for true capillary condensation.

Many investigators have attempted to distinguish between water held as capillary water and water held monomolecularly or polymolecularly in cellulose. By assuming that water adsorbed by hydrogen bonding will not freeze, Magne, et al. (38) found in calorimetric studies that in viscose rayon at -13.6°C. practically all the first

25% water adsorbed was of the nonfreezing type. For cotton at 12.8°C. all the water up to 6.4% was of the nonfreezing type. Proof of the existence of bulk water in wood pulp fibers was obtained recently by Van den Akker and Hardacker (39). They found that by application of high pressure it is possible to squeeze liquid water out of a spruce pulp fiber which is in equilibrium with air at 69% relative humidity and 22°C. (about 8% moisture content). The pressure applied was up to 20 kgf./mm.^{2} with visible droplets at 4 kgf./mm.^{2} They did not observe any bulk water if the spruce fiber was in equilibrium with air at a relative humidity lower than 69% R.H. and in other fibers did not observe bulk water even when these fibers were conditioned at 90% R.H. Most recent reviews (40, 41) do not consider capillary condensation to be important in cellulose below 70% R.H.

In the present study, it has been shown that sorbed water transport was significant even at 40% R.H. for the paper and regenerated cellulose samples. It seems very unlikely that sorbed water transport by capillary forces would be significant at this low relative humidity. It is possible that at 70% R.H. the cellulose structure is sufficiently swollen with sorbed water that one has bulk water flow due to capillary forces. In a study of the permeation of a regenerated cellulose film by oxygen in the presence of water vapor, Pilar (42) found a very rapid increase in the permeability coefficient above a relative humidity of 70%. The transition from a slow increase in the permeability coefficient of oxygen with relative humidity to a very rapid increase above 70% R.H. could be attributed to the presence of bulk or capillary water through which the oxygen could diffuse. Hermans (43) found that glycerin would not diffuse into a model regenerated cellulose filament unless the water content of the filament was greater than 13-15%, this being the equilibrium concentration at 65% R.H. Hermans claims that this is about the same moisture content at which the uptake of chemically bound water is finished.

The high permeability coefficient of the cellulose acetate film even at low relative humidity cannot be explained in terms of the capillary condensed water theory. The transport of water vapor through cellulose acetate is clearly in the sorbed phase because even helium has a much smaller permeability coefficient through a cellulose acetate film. It does not appear likely that the presence of plasticizer molecules should affect transport by capillary flow. Jayme and Balser (44) state that small plasticizer molecules such as glycerin do not affect the basic structure of regenerated cellulose. In the present study it was found that at a given relative humidity the permeability coefficient for a glycerin-plasticized regenerated cellulose film was about 30% higher than for a film with the glycerin removed.

It is difficult to determine what the net effect of a temperature change on the permeability coefficient should be if capillary condensed flow were controlling. Since viscosity decreases with increasing temperature, the resistance to viscous flow would be less at higher temperatures. But the surface tension of water decreases with increasing temperature, thereby decreasing the force causing capillary flow. Thus, one cannot deny the possibility of capillary condensed flow just from the observed temperature dependence of the permeability coefficients.

In summary, it does not appear likely that all the sorbed water transport through paper can be attributed to capillary condensed water flow. This phenomenon probably becomes important only at relative humidities higher than those reached in this study.

SURFACE DIFFUSION

In surface adsorption theories, cellulose is considered to have a large amount of internal surface which contains residual valences or polar groups which can strongly adsorb water. Much of this surface is not available for adsorption until a strong swelling agent such as water breaks some of the hydrogen bonds which hold the cellulose

polymer chains together. Support for the theory that most water is held on cellulose at surface adsorption sites can be found from nitrogen adsorption experiments on water-dried and WAN-dried cellulose. A WAN-dried cellulose is a cellulose that was first completely swollen in liquid water, had the water replaced with an alcohol, had the alcohol replaced by n-pentane, and was finally flash dried to remove the pentane. The surface area according to Brunauer-Emmett-Teller (B.E.T.) theory analysis gives for nitrogen adsorption on a water-dried cellulose a surface area of 0.5-1.0 $m.^2/g.$, whereas the WAN-dried cellulose gives 50-200 $m.^2/g.$ (45). The latter value is quite close to the value calculated from the water-vapor adsorption isotherm. Thus, the swelling action of water is thought to expose the internal surface and adsorption can take place on primary sites or in multilayers.

Vollmer (3) was able to correlate his sorbed water-vapor permeability data through paper samples by assuming that the sorbed water flux was proportional to the product of the sorbed concentration and the concentration gradient. It appears that Vollmer's basis for using this product comes from Babbitt (11) [his Equation (32)] who gave the following equation for the diffusion of a mobile monolayer:

$$Nu = - \frac{kT}{C_R} N \frac{dN}{dz} \qquad (31)$$

where Nu is the flux and N is the number of molecules adsorbed on the surface per unit volume of the medium. Equation (31) follows if the equation for the spreading pressure of a mobile monolayer [Equation (3)] is substituted into Babbitt's equation relating spreading pressure to the velocity of the adsorbed film:

$$\frac{d\phi}{dz} = -C_R u. \qquad (5)$$

In a subsequent article, Babbitt (46) stated that he had intended the coefficient of resistance, C_R, to be the resistance per molecule rather than the resistance per unit

volume. On the assumption that the resistive force per molecule is a constant independent of the number of molecules adsorbed, his fundamental dynamic equation becomes

$$\frac{d\phi}{dz} = -C_R Nu, \tag{32}$$

and substitution of the spreading pressure for a mobile monolayer leads to

$$Nu = \frac{kT}{C_R} \frac{dN}{dz} . \tag{33}$$

This is simply Fick's first law of diffusion. Since a mobile monolayer is the two-dimensional analogue of a perfect gas, Babbitt says it is not surprising to find that Fick's law should be applicable. But on analyzing surface diffusion data, Babbitt found that surface diffusion equations developed in his first article for ideal localized adsorption and B.E.T. adsorption described experimental data better than did equations using Equation (32) as the fundamental dynamic equation. He suggests that Equation (5) amounts to assuming that the binding force between adsorbed molecules and the adsorbing surface varies as $1/N$. Since, in many real systems, the heat of adsorption decreases with increasing adsorbed concentration in roughly a linear manner, Babbitt suggests this as the reason why better agreement was found when Equation (5) was used rather than Equation (32). That this assumption is inherent in Equation (5) has not been acknowledged by the investigators (4, 12, 13) who have used it as a starting equation for the development of surface diffusion equations.

Vollmer obtained a straight-line relationship when he plotted P_s versus the adsorbed concentration times the gradient of the adsorption isotherm. If his basic equation is

$$N_{As} = D^* c_s \frac{dc_s}{dz} = D^* c_s \frac{dc_s}{dp_A} \frac{dp_A}{dz} , \tag{34}$$

rearrangement gives

$$N_{As}/(dp_A/dz) = P_s = D^*c_s \frac{dc_s}{dp_A} \qquad (35)$$

and $\underline{D}^*$ is the slope of $\underline{P}_s$ versus $\underline{c}_s(d\underline{c}_s/d\underline{p}_A)$. Even though the sorbed vapor-permeability coefficients determined in the present study had the same dependence on relative humidity as Vollmer's data, a plot of $\underline{P}_s$ versus $\underline{c}_s(d\underline{c}_s/d\underline{p}_A)$ did not give a good linear relationship. Vollmer's plot extended over only a small range of relative humidities, and since the product $\underline{c}_s(d\underline{c}_s/d\underline{p}_A)$ is very sensitive to the shape of the adsorption isotherm, it is probably fortuitous that Vollmer obtained such a good linear relationship. If $\underline{D}^*$ is calculated for Sample S-4 at different temperatures, it is found to be strongly dependent on the temperature. This is not in agreement with the assumption of a mobile monolayer.

Rounsley (4) derived an equation for the sorbed transport of water vapor through paper that related the observed flux to the partial pressure of water vapor and certain constants in an adsorption isotherm equation. He assumed that Babbitt's dynamical equation [Equation (5)] was applicable and that the spreading pressure was given by Equation (4) (ideal localized monolayer).

He further assumed, and this distinguishes his derivation, that only the molecules adsorbed above the first layer are mobile. This assumption was made because the first water molecules adsorbed on cellulose are adsorbed with a large heat effect and bound by strong hydrogen bonds. The number of molecules adsorbed above the first layer could be evaluated from a multilayer adsorption equation derived by Rounsley (47). The final expression for sorbed vapor transport is

$$N_{As} = \frac{kTN_oC}{p_oC_R}\left[\frac{x(x - x^n)}{[1 + (C - 1)x]^2(1 - x)^2}\right]\frac{dp_A}{dz} \qquad (36)$$

where x is the relative pressure of water vapor and C and n are constants in Rounsley's multilayer adsorption equation corresponding to the partition function for adsorption and the maximum number of layers adsorbed, respectively. The complete derivation of this equation is given in Appendix III. The term $[1 + (C - 1)x]$ is not squared in Rounsley's final equation because an algebraic mistake was made in its derivation.

A necessary but not sufficient criterion for this equation to describe the adsorbed diffusion process is that for a small pressure difference a plot of the flux divided by the pressure drop across the sheet (P_s) versus the quantity inside the large parentheses be linear. The results of such calculations when $C = 14$ and $n = 6$ are given in Appendix III for Sample S-4. The absolute temperature and saturated vapor pressure are included in the abscissa term to determine the temperature dependence of C_R. At the lower relative pressures, Equation (36) does not predict a fast enough rise in the sorbed water-permeability coefficient, but at about 70% R.H. it begins to predict too fast a rise. The coefficient of resistance term is a strong function of temperature as well as being a complex function of adsorbed concentration. Thus, Equation (36) does not appear to be very useful in predicting adsorbed flow of water vapor through paper. That this equation does not hold is not surprising when one considers the assumptions made in deriving it. Doubts have already been raised about the use of Equation (5) as a starting equation. Equation (4) gives the spreading pressure for ideal localized adsorption, yet Rounsley's derivation assumes that the adsorbed molecules in the first layer are immobile.

Stamm (48) proposed that the attractive force of cellulose for water, as indicated by the differential or isoteric heat of adsorption, increases exponentially with a decrease in moisture content and presumably with the distance of the water molecule from the adsorption sites. Water held in successive polymolecular layers at the

surface will be held by rapidly decreasing forces and hence will be freer to move to adsorption sites farther into the film. This would lead to rapidly increasing diffusion coefficients of sorbed water in cellulose with increasing moisture content. Stamm did not attempt to correlate his sorbed water diffusion data with differential heats of adsorption. Perkinson (49) has proposed an empirical relationship based on the assumption that the activation energy for surface diffusion is related to the differential heat of adsorption by the following equation:

$$D_s = D^o \sqrt{T} \exp(\beta \Delta H/RT) \qquad (37)$$

where D^o is an arbitrary constant, ΔH is the differential heat of adsorption, and β is the proportionality factor between the activation energy and the heat of adsorption. The $\sqrt{T}$ factor was added arbitrarily because it improved his correlations. Using differential heats of adsorption for regenerated cellulose given by Guthrie (50), Equation (37) was applied to the diffusion coefficients for Sample R-2 given in Fig. 13. A good empirical fit could be obtained at a given temperature for a sorbed water concentration between 7 and 13 grams per 100 grams of cellulose. But Equation (37) did not predict the rapid rise in the diffusion coefficient at a given sorbed water content with increasing temperature. If the differential heat of adsorption is a measure of the mobility of adsorbed water molecules, one would expect this could be used to explain the difference in behavior between the regenerated cellulose and cellulose acetate films. But according to Guthrie (50), the differential heat of adsorption at zero percent moisture content for cellulose acetate is the same as for regenerated cellulose. Thus, one would not expect the high sorbed vapor permeability coefficient for cellulose acetate at zero percent relative humidity if the differential heat of adsorption was a measure of the mobility of adsorbed molecules.

It is apparent that the analysis of surface diffusion phenomena is not sufficiently advanced to permit predicting with any confidence the dependence of surface diffusion

on temperature and concentration in the multilayer region. Very little data have been obtained in the multilayer region because for most systems where surface diffusion is significant, one reaches the onset of capillary condensation as multilayer adsorption starts. For systems studied so far, the diffusion coefficient based on Fick's law has been constant or increased slightly with adsorbed concentration in the region above complete monolayer coverage (1). The present study showed that the sorbed water diffusion coefficient in cellulosic materials increases rapidly with increasing sorbed water concentration even below the region where capillary condensation is expected to occur. Surface diffusion theory does not explain the difference in behavior between the regenerated cellulose and cellulose acetate films. Nor does it explain the effect of the presence of a plasticizer in the regenerated cellulose films. These observations are not, however, sufficient evidence to preclude the presence of significant surface diffusion in the cellulose-water vapor system. More data on systems where movement by surface diffusion in multilayers is known to occur must be obtained to compare with the results of the present study.

SOLID SOLUTION DIFFUSION

In the treatment of sorption by solution theories, cellulose is treated as a system comprised of ordered regions embedded in a matrix of disordered regions, and sorption is considered to be a process of solution of water in the disordered regions. The mixing of water in these regions is analogous to the dilution of sulfuric acid. The first sorbed molecules are tightly held as water of hydration and further dilution leads to molecules less strongly held by the sorbate. This concept is based on the fact that, for some polymeric systems such as cellulose nitrate-acetone, a solution of the adsorbent occurs at high relative pressure of the sorbate (51).

Since the mobility of the polymer chain segments is thought to control the sorbed vapor diffusion process in polymer films, anything which affects this mobility

affects the diffusion process. An increase in temperature will cause increased thermal motion of polymer chain segments, leading to the Arrhenius temperature dependence of the diffusion coefficient given in Equation (30). If there is interaction between the sorbed molecules and the polymer, the diffusion coefficient for that system usually increases with increasing sorbate concentration. The interaction is said to produce a "plasticizing" effect leading to augmented chain mobility. This can be caused by breaking hydrogen bonds or by weakening van der Waals forces of attraction between polymer chain segments. This augmented chain mobility can be produced by adding a specific plasticizing agent to the polymer film or it can result from the self-plasticizing effect of the diffusing vapor.

When an organic vapor diffuses through a polymer film which would dissolve if placed in the organic liquid, it has been found that the diffusion coefficient calculated from Fick's first law of diffusion can be empirically related to the sorbed vapor concentration by

$$D_{sf} = D_{sf_o} \exp(\psi c_s) \tag{38}$$

where D_{sf_o} is the diffusion coefficient at zero sorbed vapor concentration and ψ is a proportionality factor. The diffusion coefficient increases rapidly with sorbed vapor concentration because the sorbed molecules solvate the polymer molecules. Segmental mobility of the polymer chains increases with increasing concentration until the film is dissolved in the sorbate. Prager and Long (52) investigated the effect of sorbate concentration on the diffusion coefficients for six hydrocarbons (propane, n- and isobutane, and n-, iso-, and neopentane) diffusing through polyisobutylene at 35°C. They found an exponential dependence of the diffusion coefficient on sorbate concentration in all cases. The degree of branching of the diffusing molecule had a much greater effect on the diffusion coefficient than did molecular size. They reasoned that this supported the "hole" theory of diffusion. Hansen (53) obtained

diffusion coefficients for methanol, ethylene glycol monomethyl ether, chlorobenzene, and cyclohexanone diffusing through polyvinyl acetate at 25°C. The diffusion coefficients all increased in an exponential manner with sorbate concentration. The shape and size of the diffusing molecules were more important than any hydrogen bonding tendencies of the sorbates. Hansen attributed the effect of sorbate concentration to plasticization of the polymer chains.

McCall (54) studied the diffusion of benzene and n-hexane into ethylene polymer films. He found that his diffusion data could be represented by Equation (38). Nuclear magnetic resonance studies had shown that the polymer chains in the amorphous regions of the ethylene film had considerable mobility. McCall postulated that the diffusion of sorbate molecules proceeded in the "liquidlike" amorphous regions of his film in a manner analogous to liquid diffusion. Since the sorbate molecules solvated or plasticized these amorphous regions, the diffusion coefficient increased with increasing concentration. McCall suggested investigating the effect of sorbate concentration on polymer chain mobility in the amorphous regions of ethylene polymers by nuclear magnetic resonance techniques. Such information has not been forthcoming.

The diffusion coefficients of many other systems can be represented by Equation (38). There is no theoretical justification for this particular form of the equation, although McCall (54) states that the exponential dependence implies that the activation energy for diffusion varies linearly with concentration. The diffusion coefficients for paper Sample S-4 and regenerated cellulose Sample R-2 given in Fig. 12 and 13 could also be represented by Equation (38) at the lower sorbed vapor concentrations. Other observations in the present study can also be interpreted in terms of solid-solution diffusion theory.

Plasticizers such as glycerin have been found not to affect the basic structure of cellophane, while greatly increasing the flexibility and elastic properties of

the film. Hansen, Marker, and Sweeting (55) have investigated the effect of glycerin, water, and other small molecules on the elastic modulus of regenerated cellulose films. From their experiments, they concluded that the softening or plasticizing effect is not dependent on the degree of swelling alone, but that there is a specific effect of the added molecule. Their experiments supported the view that the softening action results from partial disruption of the hydrogen-bonded structure of cellulose. The increased flexibility and elasticity can be associated with fewer hydrogen-bond cross-links between cellulose polymer chains. If flexural rigidity is taken to be a measure of the softness of a paper sheet, McPherson (56) showed that there was an equivalence of two molecules of water to one of glycerin in affecting the softness of a paper sheet. The fact that one curve can be used to relate the flexural rigidity and various combinations of glycerin and moisture strengthens the argument that glycerin and water act similarly in their softening mechanism.

The bulky acetyl groups in cellulose acetate prevent the close association of neighboring cellulose chains, and the hydrogen bonds formed between chains are less numerous than in regenerated cellulose. Cellulose acetate fibers are, in general, "softer" and more flexible than regenerated cellulose fibers (57). The more numerous hydrogen-bond cross-links between cellulose polymer chains may explain why the sorbed water permeability coefficients at low relative humidities are so much higher for cellulose acetate than for regenerated cellulose and paper. The sorbed water molecules would also be expected to plasticize the cellulose acetate film, but since cellulose acetate is less hygroscopic than cellulose, the effect would not be as evident. If one compares the increase in permeability coefficient with increasing sorbed water concentration, however, one will find that the permeability coefficients for cellulose acetate increase as quickly with sorbed water concentration as the permeability coefficients for regenerated cellulose.

The temperature dependence of the diffusion coefficients calculated for paper Sample S-4 is not inconsistent with the mechanism of solid-solution diffusion. The activation energy for diffusion calculated from the slopes of the lines in Fig. 15 has a value that compares well with activation energies found for most polymer-gas systems. Not too much significance should be assigned to this value, however, since it is probable that there will be interaction between the temperature and concentration dependence of the diffusion coefficient.

A very rapid increase in the diffusion coefficient with increasing sorbate concentration has been found for a variety of systems which have other characteristics in common with the cellulose-water system. Spencer and Ibraham (58) obtained diffusion coefficients for water vapor diffusing through polyvinyl alcohol. At low concentration of sorbed water, they found the data could be represented by an exponential dependence of the Fickian diffusion coefficient on concentration. Fish (59) and Hanson (60) have shown that below 15% moisture content the diffusion coefficient for the water-vapor sorption in starch granules can be represented by Equation (38). The diffusion coefficients for water vapor diffusing through nylon films also increase rapidly with sorbed moisture content (31).

The physical picture for the solid-solution theory of water-vapor transport through cellulose can be summarized in the following manner. Dry cellulose films or fibers consist of dense, nonporous networks which do not dissolve permanent gases to any extent and are nearly impermeable to liquids or vapors which do not interact with or swell cellulose. The more rapid diffusion in swollen networks is associated with the plasticizing action of the water or swelling agent. The lower attractive forces between chains result in more rapid Brownian motion of segments of the chains and therefore more rapid diffusion. The plasticizing action is also associated with the greater flexibility and softness of swollen films or fibers. This same description of the diffusion process was given by Howsmon (51) in 1954.

EMPIRICAL EQUATION FOR SORBED WATER TRANSPORT IN PAPER

The transport of water vapor through paper in the sorbed phase is a complex phenomenon that presently cannot be well represented by any equation derived from theoretical considerations. The calculation of diffusion coefficients for the diffusion of sorbed water through cellulose is of doubtful validity since the system so obviously does not obey Henry's law. The results presented in Fig. 8, however, suggest that a useful empirical equation relating the sorbed vapor-permeability coefficient to the relative humidity could be obtained which might apply generally to all papers. Assuming that the transport of water vapor in the sorbed phase proceeded independently of that in the gas phase, the sorbed vapor-permeability coefficients for paper Samples S-1, S-2, and S-4 were calculated. The gas-phase flux was calculated assuming normal diffusion. The results of these calculations are shown in Fig. 16. Vollmer's (3) sorbed vapor permeability coefficients for two of his paper samples are included in Fig. 16. His paper samples had an apparent density of about 1.0 g./cm.^{3}, and the permeability coefficients were determined at 20°C. It can be seen from Fig. 16 that the magnitude of P_s and its dependence on relative humidity is similar for many different papers. The data in Fig. 16 were correlated by the following empirical equation:

$$P_s = 2 \times 10^{-16} \exp(8x) \qquad (39)$$

where x is the relative vapor pressure of water. In the range 0 to 70% R.H., Equation (39) correlates the sorbed vapor-permeability coefficient of all samples studied quite well. It apparently applies to a variety of papers over the temperature range 20 to 50°C.

That the sorbed vapor-permeability coefficients for paper are apparently independent of temperature if compared at the same relative humidity is the result of a

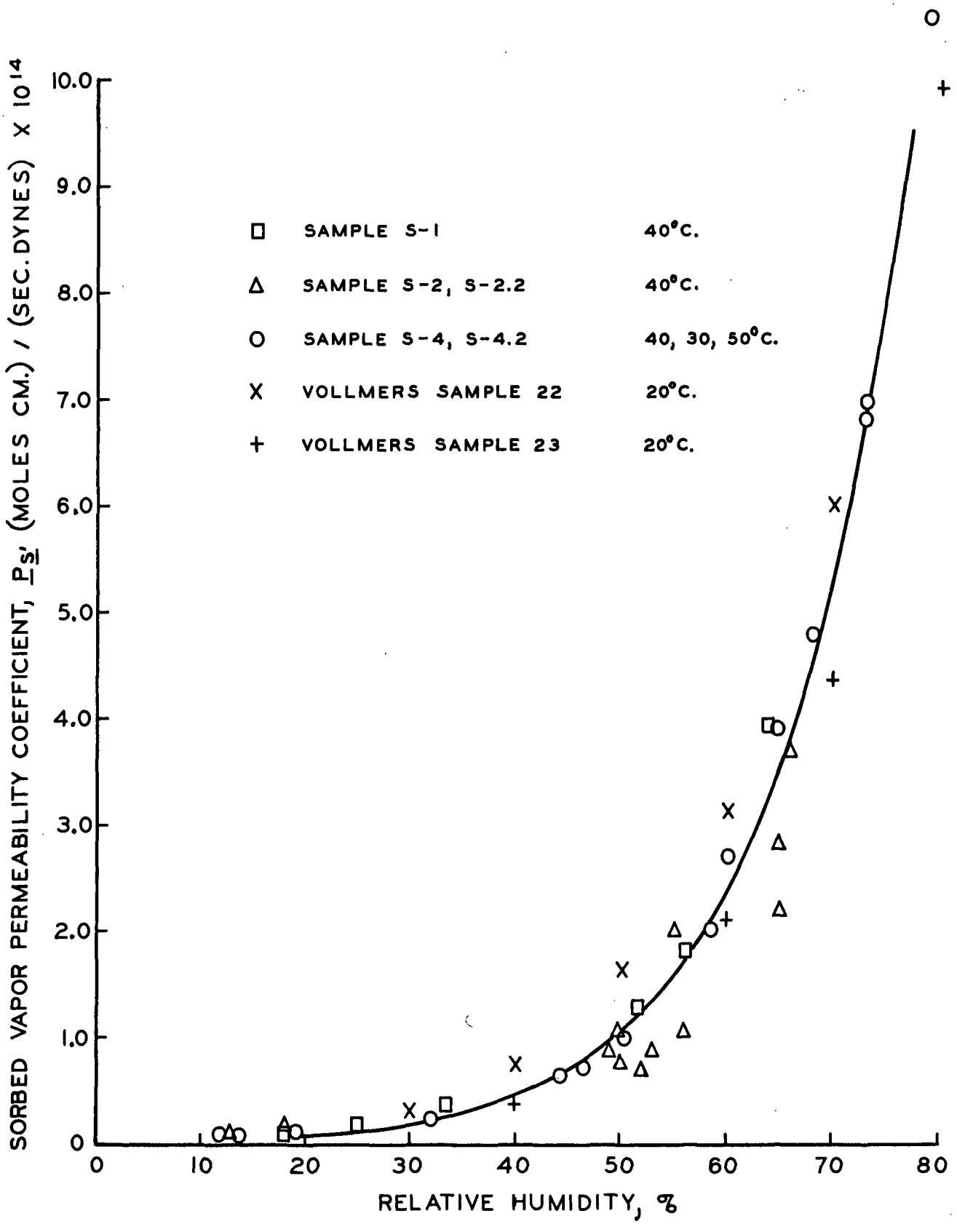

Figure 16. Empirical Equation for Sorbed Vapor Permeability Coefficients in Paper

fortuitous balancing of two effects. As the temperature is increased, the flux for a given sorbed vapor concentration gradient increases because of a positive activation energy for diffusion. As the temperature is increased the water-vapor pressures at the two surfaces of the paper sample must be increased to maintain the same sorbed vapor concentration gradient through the sample. At a given sorbed vapor concentration gradient the magnitude of the difference in water-vapor pressure across the sample increases with increasing temperature because of the negative heat of sorption of water vapor on cellulose. Since the sorbed vapor-permeability coefficient is simply the flux divided by the vapor-pressure gradient, the increase in flux with increased temperature for a given sorbed vapor concentration gradient is balanced by an increase in the partial pressure difference required to maintain that sorbed vapor concentration gradient.

To see mathematically how these effects could tend to balance one another, we assume that the water-vapor adsorption isotherm can be approximated by a straight line. The slope of this line is generally called the solubility coefficient, $\underline{S}$, and its temperature dependence has been found to be related to the heat of adsorption by (31):

$$S = \frac{c_s}{p_A} = S_o \exp(-\Delta H/RT) \tag{40}$$

From Equation (27)

$$P_s = D_s S \tag{41}$$

so that

$$P_s = D_{s_o} S_o \exp[-(\Delta E_D + \Delta H)/RT]. \tag{42}$$

It was found for paper Sample S-4 that $\Delta \underline{E_D} \cong 13$ kcal./mole. For the permeability coefficient to be independent of temperature $\Delta \underline{H}$ should be -13 kcal./mole. For the water vapor-cellulose system $\Delta \underline{H}$ is quite close to this value ($\cong$ -10 kcal./mole) and hence it is not surprising that the permeability coefficient is apparently independent of temperature if compared at the same moisture content or relative humidity.

CONCLUSIONS

The importance of the transport of water vapor through paper in the sorbed phase has been established. The importance of this mode of transport relative to gas-phase transport depends upon the moisture content of the sample. For an ordinary kraft linerboard at 60% R.H., about 15% of the diffusional transport of water vapor is in the sorbed phase. For less porous papers, sorbed water transport is the controlling mechanism of transport at relative humidities above 30%.

At relative humidities above 70%, it is possible that capillary condensed flow becomes the controlling mechanism of water transport. Below this relative humidity, the mechanism is either one of surface diffusion or solid-solution diffusion. Equations derived from different models based on the spreading pressures of adsorbed monolayers and multilayers did not account for the rapid increase in sorbed water diffusion coefficient with increasing moisture content. If it was assumed that each succeeding adsorbed layer was much more mobile than the one under it, the surface diffusion model could account for the rapid increase in the diffusion coefficient. But surface diffusion theory did not explain the effect of plasticizer in the regenerated cellulose film nor the different water-vapor permeation behavior of cellulose acetate and regenerated cellulose.

Below 70% R.H., the sorbed water-diffusion process seems to be best characterized as proceeding in the amorphous regions of cellulose by a solid-solution mechanism. The rapid increase in the sorbed vapor-diffusion coefficient can be associated with the plasticizing action of water. The lower attractive forces between cellulose polymer chain segments result in more rapid Brownian motion of the chain segments and therefore more rapid diffusion. None of the observations of this study were inconsistent with the solid-solution theory of transport.

Sorbed water-vapor diffusion (excluding capillary flow) is important during the last stage of drying of fairly dense papers. The results of this study also suggest that a drying system which would lead to thin shells of cellulose at very low moisture content around the fibers or on the surface of the paper could negatively affect the drying rate because of the very low permeability of water vapor through cellulose of low moisture content.

Sorbed water diffusion is probably very important in the rewetting of glassine before calendering operations. It would also be important in moistureproofed papers and packages where exposure to high humidities could lead to sorbed water diffusion in fibers protruding into and through the protective coatings.

An empirical equation which related the sorbed vapor-permeability coefficients to relative vapor pressure was obtained. This equation correlated the data of the present study very well over the relative humidity range 0 to 70% R.H. The equation also correlated Vollmer's sorbed water-vapor data quite well and seems to be generally applicable to paper over the temperature range 20 to 50°C. The equation shows the importance of determining the WVP coefficient of cellulosic materials at the particular relative humidity of interest.

FUTURE WORK

To conclude with certainty that the sorbed vapor transport through paper is controlled by the thermal motion of polymer chain segments would require investigations in several areas.

It may be possible with more refined analysis of nuclear magnetic resonance data to determine the effect of adsorbed moisture on the mobility of cellulose polymer chains. Nuclear magnetic resonance data are being used to differentiate various vibrational modes of hydrogen-bonded water. It may be possible to distinguish the different ways water is held in cellulose using these techniques. The presence of molecularly held water and bulk-held water could presumably be distinguished.

The effect of concentration and temperature on surface diffusion in multilayers should be investigated. A porous medium which has a very narrow pore size distribution and which strongly adsorbs the vapor being studied should be used. A constant total pressure system would allow the pores to be relatively large while not masking the effect of surface diffusion transport.

A model for solid-solution diffusion which postulated a bimolecular activated complex could be formulated. Erying's absolute reaction rate theory could be used to derive expressions for the temperature and concentration dependence of the diffusion rate.

NOMENCLATURE

A = cross-sectional area of test section of diffusion cell, $cm.^2$

a = activity, moles/cc.

C = coefficient in Rounsley's multilayer adsorption equation

C_R = coefficient of resistance in Babbitt's dynamic equations

c_s = sorbed molar concentration, moles/cc.

D_{AB} = normal diffusion coefficient, $cm.^2/sec.$

D_{KA} = Knudsen diffusion coefficient, $cm.^2/sec.$

D_s = sorbed vapor diffusion coefficient based on chemical potential driving force, $cm.^2/sec.$

D_{sf} = Fick's law sorbed vapor diffusion coefficient, $cm.^2/sec.$

ΔE_D = activation energy for diffusion, kcal./mole

ΔH = differential or isoteric heat of adsorption or solution

h = Planck's constant

K = initial slope of vapor pressure-concentration curve

k = Boltzmann's constant

L = geometric thickness of test sample, cm.

M, M_A, M_B = molecular weight

N, N_1, N_u = total number of molecules adsorbed, number in first layers, and number above first layer, respectively

$\vec{N}_A$ = total molar flux of species A with respect to stationary coordinates, moles/sec. $cm.^2$

$\vec{N}_{Ag}$ = molar flux in gas phase, moles/sec. $cm.^2$

$\vec{N}_{As}$ = molar flux in sorbed phase, moles/sec. $cm.^2$

n = maximum number of layers adsorbed in Rounsley's multilayer adsorption equation

P_s = sorbed vapor permeability coefficient, (moles cm.)/(sec. dynes)

p = total pressure, atm.

p_A = partial pressure of species A, $dynes/cm.^2$

p_o = saturation vapor pressure of species A, dynes/cm.^{2}

R = universal gas law constant

r = radius of capillary, μm.

r_{AB} = ratio of diffusion fluxes, $\vec{N}_B/\vec{N}_A$

T = temperature, °K

u = average surface velocity of adsorbed molecules, cm./sec.

$\bar{u}_A, \bar{u}_B$ = mean molecular speed of gas molecules, cm./sec.

x = relative vapor pressure, p_A/p_o

y_{A0} = mole fraction of species A at $z = 0$

y_{AL} = mole fraction of species A at $z = L$

z = z coordinate perpendicular to plane of sample, cm.

α = $1 + r_{AB}$

β = proportionality factor between activation energy and differential heat of adsorption

γ = activity coefficient

θ = fraction of adsorption sites occupied

μ = chemical potential

ρ = mass density, g./cc.

σ = surface tension

ϕ = spreading pressure, dynes/cm.

ψ = proportionality factor in Equation (38)

Subscripts:

A,A' = gas species A and A'

B,B' = gas species B and B'

D = diffusion

e = effective; refers to the property of the porous medium

f = Fickian

g = gas phase

s = sorbed phase

ACKNOWLEDGMENTS

I wish to express my gratitude for the guidance and contributions of the members of my thesis advisory committee: Mr. S. T. Han, Dr. J. A. Van den Akker, and Dr. T. M. Grace. Their suggestions were of great value during the course of this study.

The valuable assistance of the following people is also acknowledged: Mr. B. D. Andrews for locating various pieces of equipment; Mr. S. Nagel for determining the pore size distribution of several paper samples with the mercury porosimeter; and to Mr. M. Filz and Mr. P. Van Rossum for constructing various pieces of equipment.

A special note of thanks is extended to my wife, Anna, for her patience and encouragement during the completion of this thesis and to my sons, Karl and Lars, who provided additional incentive for completing this study.

LITERATURE CITED

1. Carman, P. C. The flow of gases through porous media. New York, Academic Press, 1956. 169 p.

2. Kumins, C. A., J. Polymer Sci. Part C 10:1-9(1965).

3. Vollmer, W., Chem. Ing. Tech. 26:90-4(1954).

4. Rounsley, R. R., Tappi 47:95-8(1964).

5. Stamm, A. J., J. Phys. Chem. 60:83-6(1956).

6. Stamm, A. J., Forest Prod. J. 9:27-32(1959).

7. Thomson, W. (Lord Kelvin), Proc. Roy. Soc. Edin. 7:63(1870).

8. Volmer, M., and Adhikari, G., Z. Physik 35:170(1925).

9. Weaver, J. A., and Metzner, A. B., A.I.Ch.E. Journal 12:655-61(1966).

10. Fowler, R., and Guggenheim, F. A. Statistical thermodynamics. Chap. X. Cambridge, England, Cambridge University Press, 1960.

11. Babbitt, J. D., Can. J. Research 28, Sec. A:449-74(1950).

12. Gilliland, R. E., Baddom, R. F., and Russell, J. L., A.I.Ch.E. Journal 4:90-6 (1958).

13. Bell, W. K., and Brown, L. F., J. Phys. Chem. 72:2365-71(1968).

14. Lakshminarayanarah, N., Chem. Rev. 65:491-565(1965).

15. Matters, J. F. Counterdiffusion of carbon dioxide and nitrogen through dry and partially saturated fiber beds. Doctor's Dissertation. Appleton, Wis., The Institute of Paper Chemistry, 1965. 149 p.

16. McCarty, K. P., and Mason, E. A., Phys. Fluids 3:908-22(1960).

17. Hoogschagen, J., Ind. Eng. Chem. 47:907-13(1955).

18. Evans, R. B., III, Watson, G. M., and Truitt, J., J. Chem. Eng. Data 6:522-5 (1961).

19. Dullien, F. A., and Scott, D. S., Chem. Eng. Sci. 17:771-5(1962).

20. Reeves, H. R. Fluid flow through model wire screens and development of a micromanometer. A-291 Problem. Appleton, Wis., The Institute of Paper Chemistry, 1961.

21. Eichorn, R., and Irvine, T. F., Rev. Sci. Instr. 29:23-7(1958).

22. Lindsay, A. L., and Bromley, L. A., Ind. Eng. Chem. 42:1508-11(1950).

23. Stafsing, B. I., Svensk Papperstid. 58:392-4(1955).

24. Bliesner, W. C. A study of the porous structure of fibrous sheets used in permeability techniques. Doctor's Dissertation. Appleton, Wis., The Institute of Paper Chemistry, 1963. 200 p.

25. Wink, W. A., Mod. Pkg. 20:135-8, 162, 164(Feb., 1947).

26. Jeffries, R. J., J. Textile Inst. 51:T339-74(1960).

27. Wahba, M., J. Phys. Colloid Chem. 54:1148-60(1950).

28. Chabert, J., Bull. Inst. Textile France 124:553-608(1966).

29. Newsome, P. T., and Sheppard, S. E., J. Phys. Chem. 36:930-8(1932).

30. Scheschels, H., Chem. Ing. Tech. 28:698-702(1956).

31. Stannett, V., Szwarc, M., Shargava, R. L., Meyer, J. A., Myers, A. W., and Rogers, C. E. Permeability of plastic films and coated papers to gases and vapors. TAPPI Monograph Series No. 23. New York, TAPPI, 1932. 105 p.

32. Barrer, R. M. Diffusion in and through solids. p. 436. Cambridge, England, Cambridge University Press, 1941.

33. Hauser, P. M., and McLaren, A. D., Ind. Eng. Chem. 40:112-17(1948).

34. Wellons, J. D., III. The solution and diffusion of water (vapor) in cellulose derivatives. Doctor's Dissertation. Durham, N. C., Duke University, 1966. 94 p.

35. Stannett, V., and Williams, J. L., J. Polymer Sci. Part C 10:45-59(1965).

36. Lauer, K., Kolloid Z. 107:86-8(1944).

37. Hermans, P. H. Gels. In Kruyt's Colloid science. Vol. 2. p. 537. New York, Elsevier, 1949.

38. Magne, F. C., Portas, H. J., and Wakeham, H., J. Am. Chem. Soc. 69:1896-1902 (1947).

39. Van den Akker, J. A., and Hardacker, K. W. Unpublished work. (Cited in Bolam's Consolidation of the paper web. Vol. 1. p. 69. London, Tech. Sect. Brit. Paper & Board Makers' Assoc., 1966.)

40. Stamm, A. J. Wood and cellulose science. New York, 1964. 549 p.

41. Christensen, P. K., and Giertz, H. W. The cellulose/water relationship. In Bolam's Consolidation of the paper web. Vol. 1. p. 59-89. London, Tech. Sect. Brit. Paper & Board Makers' Assoc., 1966.

42. Pilar, F. L. The effect of sorbed vapors on the permeability of high polymer films to gases. Doctor's Dissertation. Cincinnati, Ohio, University of Cincinnati, 1957. 123 p.

43. Hermans, P. H. Contribution to the physics of cellulose fibers. New York, Elsevier, 1946. p. 21.

44. Jayme, G., and Balser, K., Das Papier 18:746-58(1964).

45. Merchant, M. V., Tappi 40:771-81(1957).

46. Babbitt, J. D., Can. J. Phys. 29:437-46(1951).

47. Rounsley, R. R., A.I.Ch.E. Journal 7:308-11(1961).

48. Stamm, A. J., Australian Pulp & Paper Ind., Tech. Assoc. Proc. 10:244-71(1956).

49. Perkinson, G. P. Flow of adsorbed gases through microporous media. Doctor's Dissertation. Cambridge, Mass., Massachusetts Institute of Technology, 1965.

50. Guthrie, J. C., J. Textile Inst. 40:T489-504(1949).

51. Howsmon, J. H. Structure-sorption relationships. In Ott and Spurlin's Cellulose and cellulose derivatives. 2d ed. Part I. p. 393-441. New York, Interscience, 1954.

52. Prager, S., and Long, F. A., J. Am. Chem. Soc. 73:4072-5(1951).

53. Hansen, C. M., Ind. Eng. Chem. Fund. 6:609-13(1967).

54. McCall, D. W., J. Polymer Sci. 26:151-69(1957).

55. Hansen, O. C., Marker, L., and Sweeting, O. J., J. Polymer Sci. 5:655-62(1961).

56. McPherson, W. H., Jr., Tappi 33:531-7(1950).

57. Wakeham, H. Mechanical properties of cellulose and its derivatives. In Ott and Spurlin's Cellulose and cellulose derivatives. 2d ed. Part III. p. 1247-87. New York, Interscience, 1955.

58. Spencer, H. G., and Ibraham, I. M., J. Polymer Sci. Part A-2 6:2071-6(1968).

59. Fish, B. P. Diffusion and equilibrium properties of water in starch. Gt. Brit. Dept. Sci. Ind. Res. Food Investigation Tech. Paper 5, 1957.

60. Hanson, T. P. Diffusion coefficient measurements for water vapor-cornstarch granule system. Unpublished M.S. Thesis. Ames, Iowa, Iowa State University, 1967.

APPENDIX I

CALCULATION OF FLUXES, PERMEABILITY, AND DIFFUSION COEFFICIENTS

The net flux of Components A and B through the medium can be calculated from a material balance around the diffusion cell. Let w_1 and w_2 be the molar flow rates into the top and bottom halves of the diffusion cell, respectively, and w_3 and w_4 be the molar flow rates out. Let y_1, y_2, y_3, and y_4 be the respective mole fractions of Component A for each of these flow rates. The experimentally measured quantities are w_1, w_2, y_1, y_2, y_3, and y_4. The overall material balance is

$$w_1 + w_2 = w_3 + w_4 \ . \tag{43}$$

The material balance for Component A is

$$y_1w_1 + y_2w_2 = y_3w_3 + y_4w_4 \ . \tag{44}$$

The material balance for Component B is

$$(1 - y_1)w_1 + (1 - y_2)w_2 = (1 - y_3)w_3 + (1 - y_4)w_4 \ . \tag{45}$$

The net flux of Component A is given by

$$N_A A = y_1w_1 - y_3w_3 \tag{46}$$

where A is the cross-sectional area of the medium. Combining Equations (43) and (44), one can obtain the following expression for w_3:

$$w_3 = [y_1w_1 + y_2w_2 - y_4(w_1 + w_2)]/(y_3 - y_4). \tag{47}$$

Substituting this expression into Equation (46) gives, after rearranging,

$$N_A A = [y_1y_4w_1 - y_2y_3w_2 + y_3y_4(w_1 + w_2)]/(y_3 - y_4). \tag{48}$$

The corresponding equation for Component B is

$$N_B A = [(y_3 + y_1 y_4 - y_1)w_1 + (y_4 + y_2 y_3 - y_2)w_2 - y_3 y_4(w_1 + w_2)]/(y_3 - y_4). \quad (49)$$

If it is assumed that the absolute value of the difference $|\underline{N_A A}| - |\underline{N_B A}|$ is small compared to the inlet flow rates, $\underline{w_1} \cong \underline{w_3}$ and $\underline{w_2} \cong \underline{w_4}$; we can then write two independent equations for calculating the flux of A in terms of the measured quantities:

$$N_A A = |y_1 - y_3| w_1 , \quad (50)$$

$$N_A A = |y_2 - y_4| w_2 . \quad (51)$$

A sample calculation to determine the flux of water vapor will be made for Run 0912-1. The raw data for this run are

Run no.	0912-1
Sample	S-4
Gases	$N_2 - H_2O$
Barometric pressure	746.5 mm. Hg
Diffusion cell pressure	749.7 mm. Hg
Pressure ahead of Rotameters R1 and R2	1000.0 mm. Hg
Total flow rate to Rotameters R1 and R2 (wet-test meter)	202.2 sec./0.1 ft.^{3}
Flow rate to Rotameter R2 (wet-test meter)	395.8 sec./0.1 ft.^{3}
Temperature of wet-test meter	80.5°F.
Temperature of air bath	40.0°C.
Temp. 2nd bath — humidity control unit 1	32.00°C.
Temp. 2nd bath — humidity control unit 2	37.92°C.
Final T/C 1 reading	10.977 mv.
Final T/C 2 reading	13.380 mv.
Check of T/C 1 calibration	10.112 mv.
Check of T/C 2 calibration	14.290 mv.
T/C 1 zero balance	0.072 mv.
T/C 2 zero balance	0.070 mv.

The calculation of molar flow rates is as follows. Let $\underline{p_b}$ be the barometric pressure, $\underline{p_v}$ the vapor pressure of water at the temperature, $\underline{T_w}$, of the wet-test meter, and $\underline{t}$ the time for one complete revolution of the wet-test meter (0.1 ft.^{3}). The dry gas flow rate through the wet-test meter, $\underline{Q}$, is given by

$$Q = 4585 p_b (1 - p_v/p_b)/[t(T_w + 427.7)] \quad (52)$$

where Q is given in mM/min., p_v and p_b in mm. Hg, t in sec., and T_w is °F. If the above experimental data are used in Equation (52), the total dry flow rate to Rotameters R1 and R2 is 32.10 mM/min. and to Rotameter R2 16.41 mM/min. By difference, R1 is 15.69 mM/min.

The moisture contents of the inlet gas streams are determined by the temperatures of the final humidity control unit baths. The thermometers used for this were checked with an NBS tested thermometer and the second one was found to read 0.10°C. too low. The water-vapor pressures corresponding to the corrected temperatures of the humidity control unit are 35.66 and 49.70 mm. Hg, respectively. Since the total pressure at the humidity control unit is 1000.0 mm. Hg, the water-vapor mole fractions through Rotameters R1 and R2 are 0.03566 and 0.04970, respectively. The total gas flow rate to the rotameters can now be calculated. Flow to R1 is 15.69/(1.000 - 0.03566) = 16.27 mM/min. and flow to R2 is 17.25 mM/min.

The compositions of the exit streams are determined from the T/C cell output readings. The final T/C cell readings are corrected for the zero balance drift:

$$\text{T/C 1} = 10.977 - 0.072 = 10.905 \text{ mv.}$$

$$\text{T/C 2} = 13.380 - 0.070 = 13.370 \text{ mv.}$$

From the calibration curves these readings correspond to water-vapor mole fractions of 0.0397 and 0.0459, respectively.

The net flux of water vapor through the sample can now be calculated. If water vapor is Component A, Equations (50) and (51) give

$$N_A A = 16.27(0.03970 - 0.03566) = 0.0656 \text{ mM/min.}$$

$$N_A A = 17.25(0.04970 - 0.04590) = 0.0654 \text{ mM/min.}$$

This is unusually good agreement. For most water vapor-nitrogen experiments the two values agreed within 10%. The flux of water vapor through the sample is small compared to the inlet flow rates so that the assumption that $\underline{w}_1 = \underline{w}_3$ and $\underline{w}_2 = \underline{w}_4$ does not lead to significant error. If the equations developed from an overall material balance are used, $\underline{N_A A} = 0.0668$ m$\underline{M}$/min., $\underline{N_B A} = -0.0377$ m$\underline{M}$/min., and the flux ratio, $\underline{r_{AB}} = -0.564$. The flux ratios calculated in this manner for other water vapor-nitrogen diffusion experiments ranged from -50 to 4. This was clearly due to the sensitivity to small experimental errors of the equations used to calculate the fluxes.

For Sample S-4, the gas-phase flux is small compared to the sorbed-phase flux and $\underline{P_s}$ can be calculated directly. The area of the test section of the diffusion cell is 45.6 cm.^{2}

$$P_s = (0.065 \times 10^{-3})/[(45.6)(0.0459 - 0.0397)(749.7)(1.33 \times 10^3)(0.00523)(60)]$$
$$= 0.74 \times 10^{-14} \text{(mole cm.)/(sec. dyne)}.$$

The relative humidities at the two surfaces of the sample for this experiment are $(0.0459)(749.7)(100)/(55.32) = 62.3\%$ R.H. and $[(0.0397)(749.7)(100)]/(55.32) = 53.8\%$ R.H. The saturated vapor pressure of water at 40°C. is 55.32 mm. Hg.

The diffusion coefficients for sorbed water transport were calculated from smoothed sorbed vapor permeability coefficients. The concentration of sorbed water vapor at a given relative vapor pressure was obtained from the adsorption isotherm of the sample. The concentration of sorbed water vapor was converted to units of moles/cc. by multiplying g. H_2O/g. cellulose by the apparent density of the sample, not by the density of pure cellulose. The diffusion coefficients calculated directly from Equation (27) or (29) give the diffusion coefficient in cm.^{2}/sec.

APPENDIX II

WATER-VAPOR ADSORPTION ISOTHERMS FOR SAMPLES S-4, R-2, AND C1

The water-vapor adsorption isotherm was determined for paper Sample S-4 by suspending a sample above different saturated salt solutions and measuring the equilibrium weight of the sample and sample holder. The sample was first dried in an oven at 40°C. and at a pressure of 0.1 atm. for three days. The final dry weight was determined by drying the sample to constant weight in a high vacuum oven (p = 26.6 dynes/cm.^{2}) at 40°C. If the sample was dried at 100°C., there was an additional 4% loss in weight. This must have been due to thermal decomposition of the sample because adsorption isotherms calculated from this weight resulted in water regains much higher than previously reported for paper. The adsorption isotherms based on the dry weight of the sample at 40°C. are given in Fig. 17. Each point represents the average of two determinations and only the adsorption part of the isotherm is given. The dashed line represents Rounsley's multilayer adsorption equation (47) when C = 14, n = 6, and B = 3.52. By varying B, the equation fits the adsorption data at the two different temperatures quite well.

The adsorption isotherm for regenerated cellulose is given in Fig. 18. The values are taken from Jeffries (26). The adsorption isotherm obtained for a cellulose acetate film by Newsome and Sheppard (29) is given in Fig. 19.

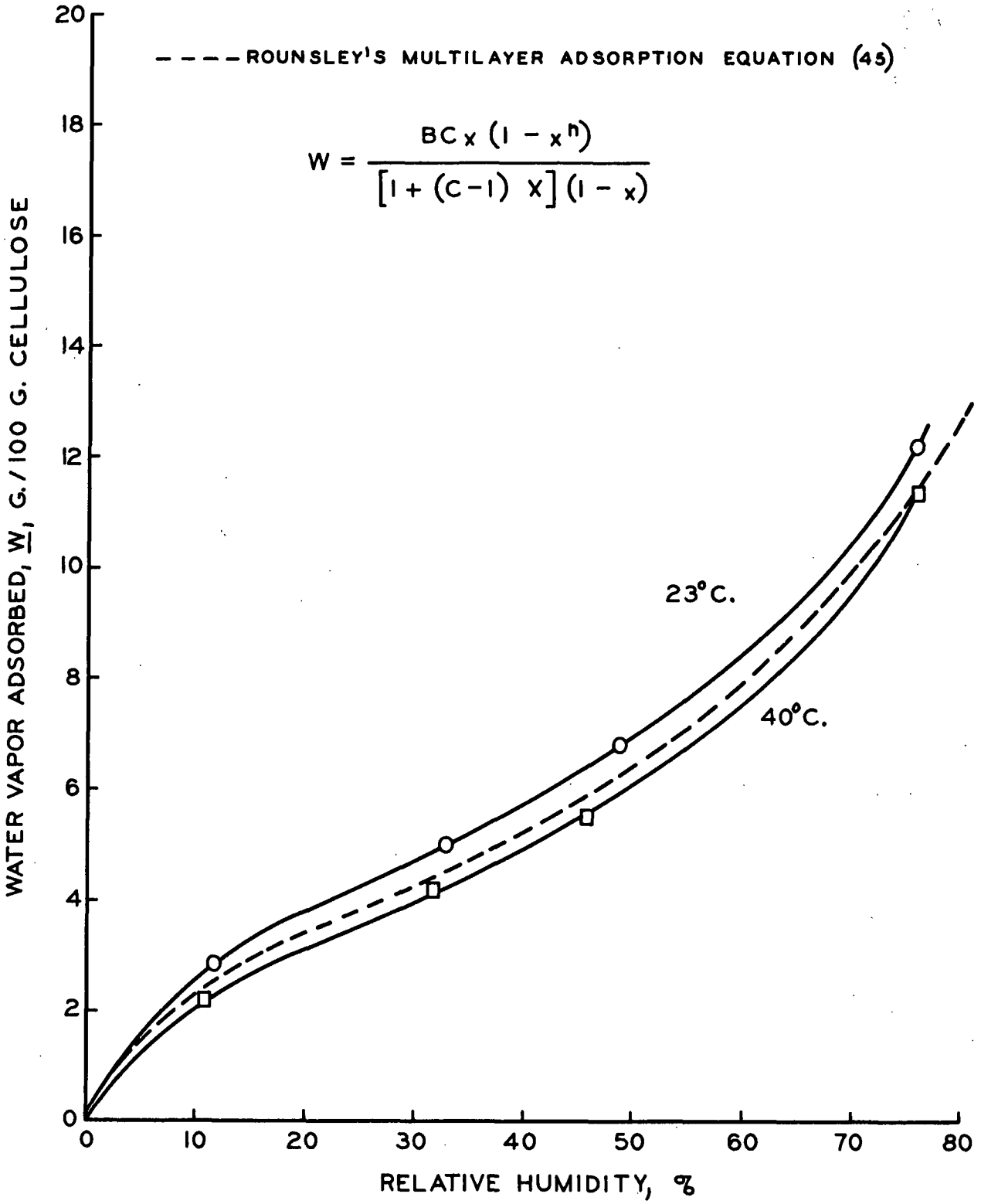

Figure 17. Water-Vapor Adsorption Isotherms for Paper Sample S-4

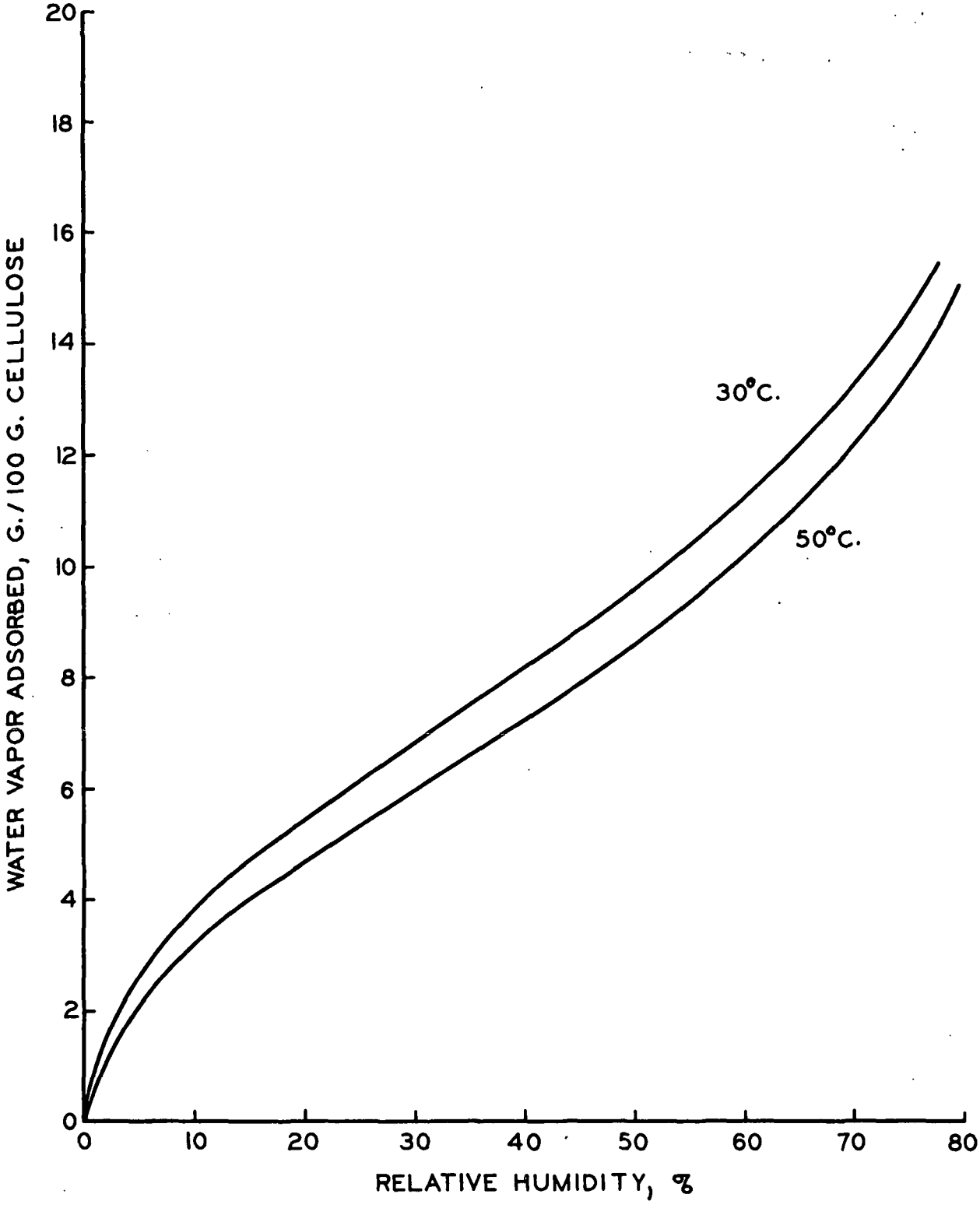

Figure 18. Water-Vapor Adsorption Isotherm for Regenerated Cellulose (26)

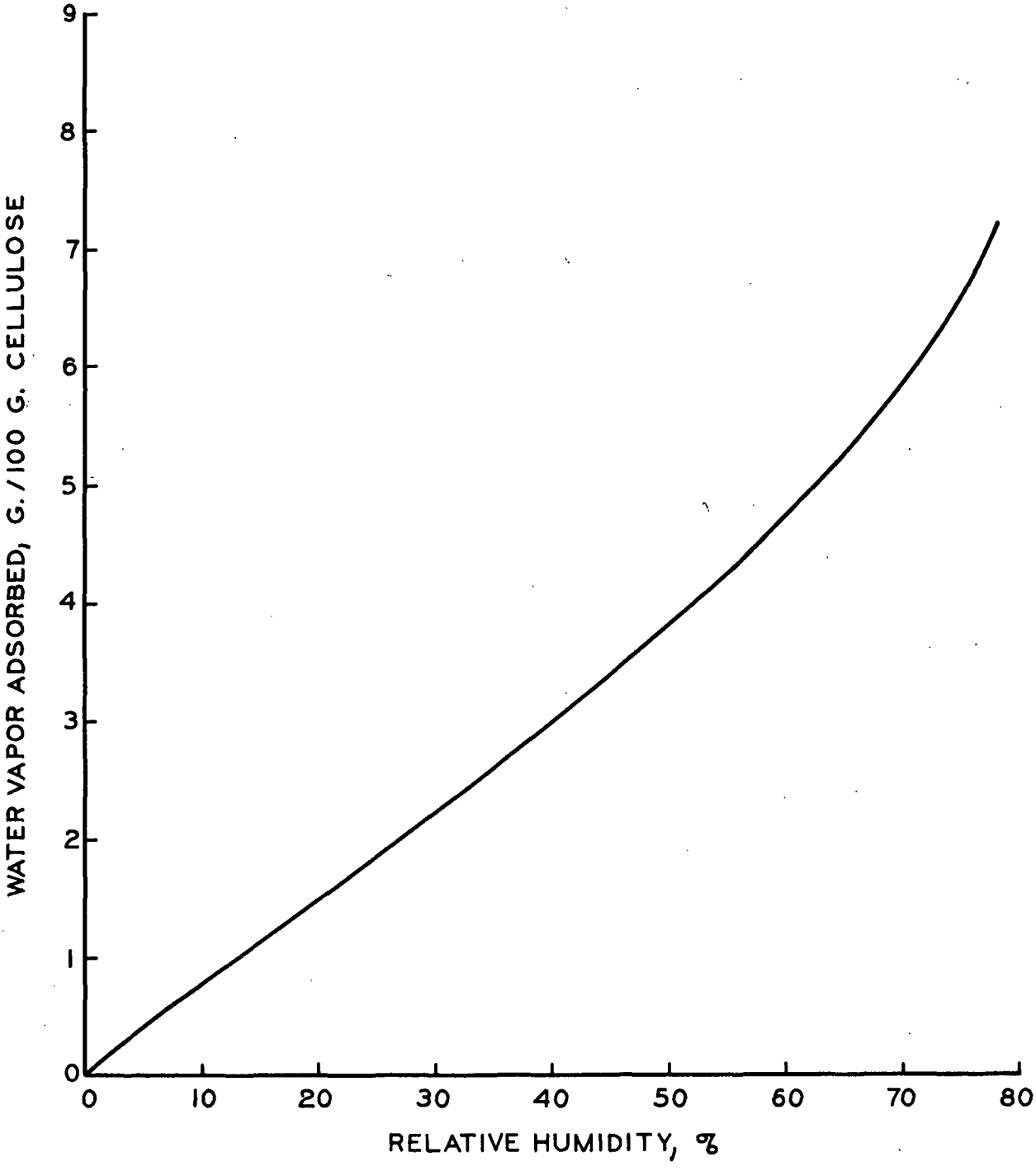

Figure 19. Water-Vapor Adsorption Isotherm for Cellulose Acetate Film (29), 40°C.

APPENDIX III

DERIVATION OF ROUNSLEY'S EQUATION

Rounsley (4) assumed that the driving force for surface diffusion was the spreading pressure. For multilayer adsorption, he found the following expression for the spreading pressure:

$$\phi = N_o RT \ln (N_o/(N_o - N_1)) \tag{53}$$

where N_1 is the number of molecules adsorbed in the first layer. This equation is identical to the equation given by Fowler and Guggenheim for ideal localized adsorption [Equation (4)]. It is also the equation given by Babbitt (11) for adsorption which obeys the B.E.T. adsorption equation.

The velocity of adsorbed molecules was related to the spreading pressure by Equation (5):

$$\frac{d\phi}{dz} = -C_R u. \tag{5}$$

Only the molecules adsorbed above the first layer, N_u, were considered mobile and the net flow was given by $N_u u$. The equation for the net flux is given by

$$N_u u = - \frac{N_u}{C_R} \frac{\partial \phi}{\partial z} . \tag{54}$$

Rounsley's multilayer adsorption equation (47) gives as the number of molecules per unit area adsorbed above the first layer

$$N_u = \frac{N_o C x(x - x^n)}{[1 + (C - 1)x](1 - x)} . \tag{55}$$

Substituting into Equation (54),

$$N_u u = \frac{N_u}{C_R} \frac{d\phi}{dp_A} \frac{dp_A}{dz} = \frac{kTN_o C}{C_R} \frac{x(x - x^n)}{[1 + (C-1)x](1 - x)} \frac{d}{dp_A} \ln \left(\frac{N_o}{N_o - N_1} \right) \frac{dp_A}{dz} . \tag{56}$$

Since $\underline{p_A} = \underline{p_o x}$,

$$N_u u = \frac{kTN_o C}{p_o C_R} \frac{x(x - x)}{[1 + (C-1)x](1 - x)} \frac{1}{N_1} \frac{N_1}{N_o - N_1} \frac{dN_1}{dx} \frac{dp_A}{dz} . \qquad (57)$$

Rounsley's adsorption equation (47) gives

$$\frac{N_1}{N_o - N_1} = \frac{Cx}{1 - x} : \qquad (58)$$

$$\therefore \quad N_1 = \frac{N_o Cx}{[1 + (C-1)x]} \qquad (59)$$

and

$$\frac{dN_1}{dx} = \frac{N_o C}{[1 + (C-1)x]^2} \qquad (60)$$

In Rounsley's derivation, the denominator in Equation (60) is not squared. If the above expressions are substituted into Equation (57), the corrected form of Rounsley's final equation is obtained:

$$N_u u = \frac{kTN_o C^2}{p_o C_R} \frac{x(x - x^n)}{[1 + (C-1)x]^2(1 - x)^2} \frac{dp_A}{dz} . \qquad (36)$$

The sorbed vapor permeability data for Sample S-4 are correlated by Rounsley's equation in Fig. 20.

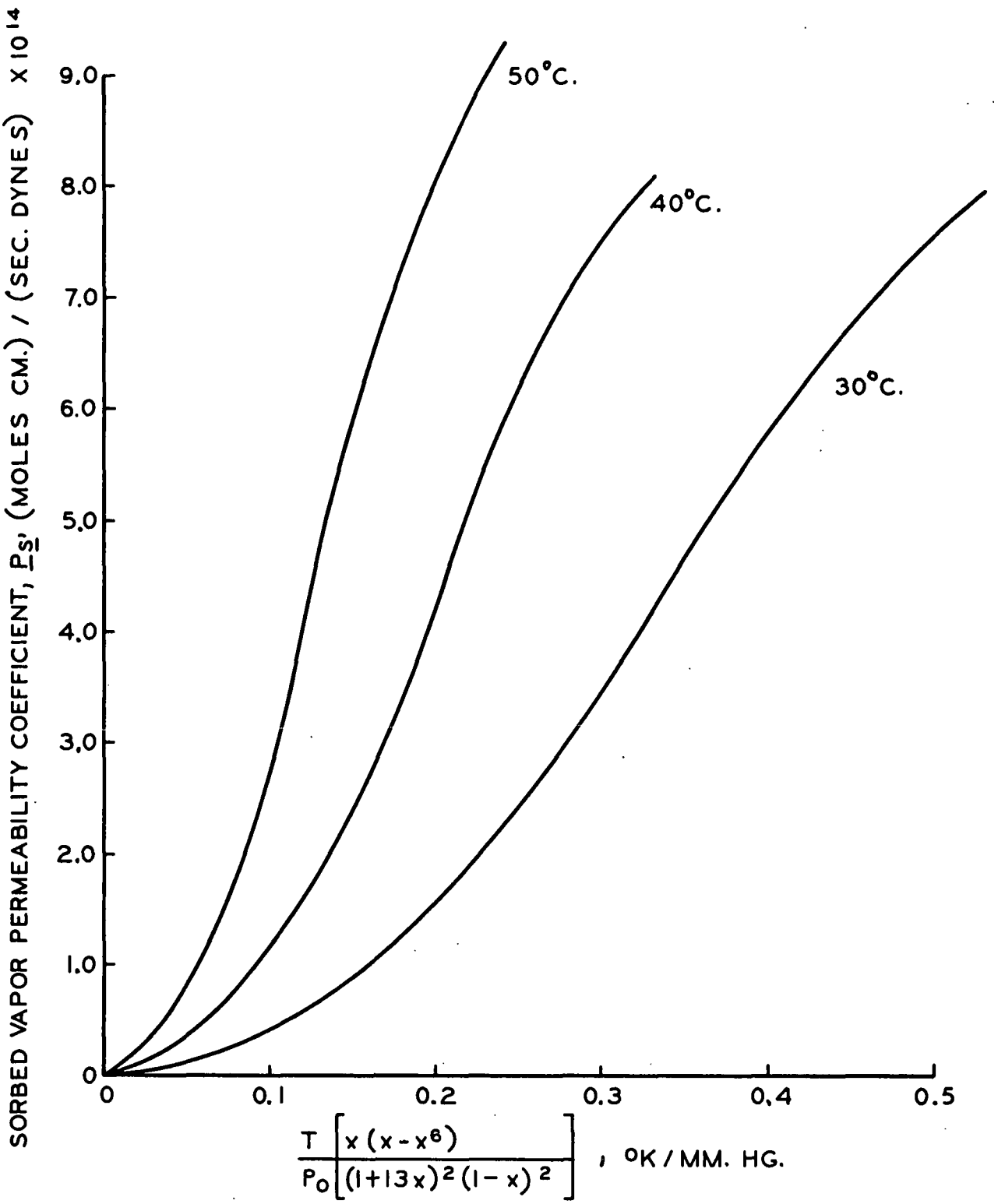

Figure 20. Correlating Sorbed Water Transport in Sample S-4 with Rounsley's Equation